

# 1 Large-scale regionalization of water table depth in 2 peatlands optimized for greenhouse gas emission 3 upscaling

4  
5 Michel Bechtold<sup>1</sup>, Bärbel Tiemeyer<sup>1</sup>, Andreas Laggner<sup>1</sup>, Thomas Leppelt<sup>1</sup>,  
6 Enrico Frahm<sup>1,\*</sup>, Susanne Belting<sup>1,2</sup>

7 [1] Thünen Institute of Climate-Smart Agriculture, Braunschweig, Germany

8 [2] Belting Umweltplanung, Quernheim, Germany

9 [\*] now at: Physikalisch-Technische Bundesanstalt, Braunschweig, Germany

10 Correspondence to: M. Bechtold (michel.bechtold@ti.bund.de)

Formatiert: Englisch (USA)

## 12 Abstract

13 Fluxes of the three main greenhouse gases (GHG) CO<sub>2</sub>, CH<sub>4</sub> and N<sub>2</sub>O from peat and other  
14 organic soils are strongly controlled by water table depth. Information about the spatial  
15 distribution of water level is thus a crucial input parameter when upscaling GHG emissions to  
16 large scales. Here, we investigate the potential of statistical modeling for the regionalization  
17 of water levels in organic soils when data covers only a small fraction of the peatlands of the  
18 final map. Our study area is Germany. Phreatic water level data from 53 peatlands in  
19 Germany were compiled in a new dataset comprising 1094 dip wells and 7155 years of data.  
20 For each dip well, numerous possible predictor variables were determined using nationally  
21 available data sources, which included information about land cover, ditch network, protected  
22 areas, topography, peatland characteristics and climatic boundary conditions. We applied  
23 boosted regression trees to identify dependencies between predictor variables and dip well  
24 specific long-term annual mean water level (WL) as well as a transformed form of it (WL<sub>t</sub>).  
25 The latter was obtained by assuming a hypothetical GHG transfer function and is linearly  
26 related to GHG emissions. Our results demonstrate that model calibration on WL<sub>t</sub> is superior.  
27 It increases the explained variance of the water level in the sensitive range for GHG emissions  
28 and avoids model bias in subsequent GHG upscaling. The final model explained 45 % of WL<sub>t</sub>  
29 variance and was built on nine predictor variables that are based on information about land

30 cover, peatland characteristics, drainage network, topography and climatic boundary  
31 conditions. Their individual effects on  $WL_t$  and the observed parameter interactions provide  
32 insights into natural and anthropogenic boundary conditions that control water levels in  
33 organic soils. Our study also demonstrates that a large fraction of the observed  $WL_t$  variance  
34 cannot be explained by nationally available predictor variables and that predictors with  
35 stronger  $WL_t$  indication, relying e.g. on detailed water management maps and remote sensing  
36 products, are needed to substantially improve model predictive performance.

37

## 38 1 Introduction

39 Greenhouse gas (GHG) emissions from organic soils can be high compared to mineral soils.  
40 In Germany, the fraction of organic soils classified as peatlands covers only 5 % of the land  
41 surface, but does account for 40 % of GHG emissions in the reporting categories 'agriculture'  
42 and 'land use, land use change and forestry' of the UN Framework Convention on Climate  
43 Change (UNFCCC) (UBA, 2012). Also other organic soils with a lower soil organic carbon  
44 content (SOC) but still meeting the definition of organic soils according to IPCC (2006) are  
45 important sources of persistently high GHG emissions (Leiber-Sauheitl et al., 2014). In our  
46 study, we also consider these soils. For simplification, we will refer in the following to the  
47 total of peatlands and 'other organic soils' as organic soils. Current estimates of GHG  
48 emissions from organic soils are fairly uncertain and reporting of most countries relies on  
49 IPCC default emission factors (EF) for  $CO_2$  emissions which are stratified for land use and  
50 climatic region, e.g.  $10 \text{ t C ha}^{-1} \text{ yr}^{-1}$  for arable land in the warm temperate zone.

51 Artificial drainage turned the function of former natural peatlands from a C sink into a C  
52 source. Experimental work with organic soils during the last two decades showed that the  
53 aerated soil pore space above the water level is one of the key variables explaining the amount  
54 of  $CO_2$  emissions (Moore and Dalva, 1993). Frequently, the water level relative to soil surface  
55 (further simply referred to as 'water level', with negative values below ground) is used as  
56 proxy for air-filled porosity, given the simplicity and availability of water level  
57 measurements. Additionally, low water levels and oxygen availability are also key drivers of  
58 nitrous oxide ( $N_2O$ ) production in organic soils (Regina et al., 1996), which increases the  
59 relevance of organic soils for climate change mitigation policy. During anaerobic conditions  
60 when water levels are at or above the land surface, substantial methane ( $CH_4$ ) emissions can  
61 occur (Levy et al., 2012).

Feldfunktion geändert

Feldfunktion geändert

Feldfunktion geändert

Feldfunktion geändert

Feldfunktion geändert

Feldfunktion geändert

62 It is postulated that the GHG-budget – the sum of the CO<sub>2</sub>-equivalents of the three main  
63 greenhouse gases (CO<sub>2</sub>, N<sub>2</sub>O, CH<sub>4</sub>) – is at minimum for annual mean water levels (annual  
64 mean further defined by the variable name WL) at about -0.05 to -0.1 m (Drösler et al., 2011).  
65 Following atmospheric sign convention, a positive budget stands for net emissions, while a  
66 negative sign indicates a net uptake of GHGs. Other parameters, as physical and chemical soil  
67 properties and vegetation, also influence the amount of the emissions, and thus weaken the  
68 relation between total GHG budget and WL.

Feldfunktion geändert

69 If available, information about the spatial distribution of WL can identify GHG hot spot  
70 regions and improve the accuracy of total GHG budgets at large scales. The application of  
71 transfer functions that relate GHG emissions to WL and potential other influencing site  
72 characteristics can refine the estimates derived from simple application of IPCC default EFs.  
73 However, in many countries and regions, as e.g. Germany and Europe, a map of WL in  
74 organic soils does not exist. The spatial availability of measured WL is much higher than of  
75 measured GHG fluxes, which suggests the use of WL as scaling parameter for upscaling  
76 GHG emissions.

77 Several methods were applied in the past to produce WL maps. Their suitability is strongly  
78 related to data availability, which very often decreases in quality and spatial density with  
79 increasing scale of the study area. Spatially-distributed process-based modeling (Thompson et  
80 al., 2009) and semi-physical statistical approaches (Bierkens and Stroet, 2007), are well able  
81 to reproduce water level dynamics in wetlands environments, including peatlands. However,  
82 they heavily rely on spatial information about the system's physical properties and boundary  
83 conditions (peat hydraulic properties, hydraulic conductivity of peat base, drainage system);  
84 data that is often only available with sufficient detail at a regional scale (Limpens et al.,  
85 2008). Despite this difficulty there are studies in which process-based models were applied to  
86 model peatland water level at large scale (national or continental). Gong et al. (2012) adopted  
87 a common SVAT model to account for the differing hydrological processes in pristine fens,  
88 pristine bogs and drained peatlands, and modeled water level fluctuations in boreal peatlands  
89 for whole Finland. But calibration and validation with data from only three mires does not  
90 allow conclusions about the accuracy and general applicability of the model. Numerous large  
91 scale hydrological wetland models are often developed with a focus on delineating wetland  
92 extent (Melton et al., 2013). TOPMODEL-based schemes (Ju et al., 2006) and more advanced  
93 large scale hydrologic frameworks (Fan and Miguez-Macho, 2011) are suited to model WL,

Feldfunktion geändert

94 but do not account for anthropogenic drainage and thus are only applicable to pristine (or  
95 nearly-pristine) peatland systems.

96 When detailed physical model input that is needed for a physically-based approach is lacking,  
97 statistical or machine learning tools represent a promising alternative (Finke et al., 2004).

Feldfunktion geändert

98 Potential predictor variables that are available at the final map scale are determined for each  
99 location with water level data and the algorithm identifies dependencies between potential  
100 predictors and target variables, as WL or other statistical values that describe water level  
101 dynamics. For areas rich in water level data, e.g. the Netherlands, residuals of the statistical  
102 model can afterwards be analyzed for spatial correlation. If this is present, it can be used to  
103 correct for spatially correlated model bias by kriging. This scheme has been applied to  
104 agricultural areas by Finke et al. (2004) and to nature conservation areas by Hoogland et al.

Feldfunktion geändert

105 (2010). Spatial interpolation approaches can include ancillary data like mapped geophysical  
106 parameters (Buchanan and Triantafilis, 2009). Statistical approaches strongly rely on both

Feldfunktion geändert

107 quantity and quality of the data on the target variable itself, i.e. the water level data. An  
108 important quality criterion for water level data from organic soils is the measurement depth. It  
109 is crucial that there is little or no hydraulic resistance by a low conductive layer between the  
110 perforated part of the monitoring well and the fluctuating water level. If the hydraulic  
111 resistance is too high, the monitoring well acts as a piezometer and water levels may  
112 substantially differ from the actual phreatic level as shown for peatlands by van der Gaast et  
113 al. (2009). If such piezometer data is part of a dataset and interpreted as phreatic water level  
114 data during model calibration, this can lead to an under- or overestimation of predicted water  
115 levels in organic soils. An underestimation of water level predictions (too dry) is discussed for  
116 Dutch modeling studies in van der Gaast et al. (2009).

Feldfunktion geändert

Feldfunktion geändert

Feldfunktion geändert

117 At present, in Germany a map on water levels in organic soils that could be used for GHG  
118 upscaling is missing. This and current efforts on improving GHG emission estimates for  
119 German organic soils were the main drivers for our study. Thus, the major goal of this study  
120 was the development of a model concept that produces a water level map at the scale of all  
121 organic soils in Germany that is specifically optimized for water level ranges to which GHG  
122 emissions react sensitively. We emphasize that the objective of our study was to regionalize  
123 annual mean water levels and not the GHG emissions themselves. The latter are influenced by  
124 more site characteristics, in particular soil properties. Furthermore, we suppose that annual  
125 mean water level is probably not the only and optimal statistical measure to describe the water

126 | level effect on annual GHG emissions. However, we are not aware of well-established  
127 | knowledge about transfer functions that relate more complex statistical measures of water  
128 | level dynamics to GHG emissions. Therefore, we here focused on the simple and frequently  
129 | applied 'annual mean water level'.

130 | In a first step, we compiled a new dataset of phreatic water level time series of organic soils  
131 | with contributions from numerous data providers. Based on this data, we developed a  
132 | modeling approach for the annual mean water level that follows the basic idea of the  
133 | statistical regionalization presented in Finke et al. (2004). However, the data situation of our  
134 | study substantially differed from their study. Our data covers only a small fraction of the  
135 | peatlands of the final map and spatial interpolation of residuals was not possible. We thus  
136 | extended their approach by:

- 137 | • including additional possible predictor variables,
- 138 | • using boosted regression trees as modeling tool to identify the influence of both  
139 | numerical and categorical variables simultaneously,
- 140 | • applying a new weighting scheme that balances out heterogeneous water level datasets  
141 | with highly variable spatial data density,
- 142 | • transforming the annual mean water level, WL, into a transformed annual mean water  
143 | level,  $WL_t$ , that shows a linear relationship with the GHG budget and optimizes model  
144 | calibration for the WL range relevant for GHG emissions, and by
- 145 | • restricting the water level regionalization to phreatic water levels of organic soils.

146 | We present a detailed analysis of the influence of the individual predictor variables on water  
147 | levels of organic soils as well as their interactions. Furthermore, the manuscript includes the  
148 | estimation of model uncertainty and possible paths of future model improvement. Finally, the  
149 | calibrated model is used to derive a map of  $WL_t$  for all organic soils in Germany, and the  
150 | regionalization results are presented.

151

Feldfunktion geändert

Formatiert: Englisch (Großbritannien)

Gelöscht: an objective

## 153 2 Dataset and Methods

### 154 2.1 Dataset of phreatic water levels in organic soils

155 Available data of phreatic water levels in organic soils are scarce. In contrast to data of rather  
156 deeply drilled observation wells of official groundwater monitoring networks, short peatland  
157 observation wells of only one or two meter length that measure the phreatic water level of the  
158 peat layer are currently not collected in central data management systems in Germany or any  
159 of its Federal States. With a comprehensive questionnaire started in 2011, we collected water  
160 level time series of organic soils from local agencies, non-governmental organizations,  
161 universities, consultants and other sources, and combined this data with water level data from  
162 our projects. Time series included manual and automatic measurements. Years with less than  
163 six measurements or data gaps of more than three months were excluded. Water level time  
164 series of each dip well were visually checked on plausible dynamics by comparing with data  
165 from neighboring dip wells and weather data time series. Based on auxiliary data and local  
166 knowledge, we further identified dip wells that reached down to the underlying aquifer. If dip  
167 wells failed these quality checks, they were removed from the dataset.

168 The final dataset comprised 7155 years of data from 53 German peatlands and 1094 dip wells.  
169 On average time series ranged over 7 years. All time series were collected at some period  
170 between the years 1988 to 2012. Data are well distributed over most of the German peatland  
171 regions and cover the three major types of organic soils (Figure 1). Compared with the  
172 distribution of the types of organic soils in Germany, the fraction of dip wells on bogs is  
173 overrepresented in the dataset by the factor of 2.5, while dip wells on fens and other organic  
174 soils are slightly underrepresented. Data also cover the common land use types (for data  
175 sources see Table 1). However, dip wells on organic soils that are neither used for agriculture,  
176 forestry or peat mining, further referred to as 'unused peatlands', are overrepresented in the  
177 dataset by a factor of 6 as data was collected more frequently and in higher spatial data  
178 density in the frame of conservation projects. The fraction of unused peatlands of the German  
179 organic soils is 6 %, and the fraction in the dataset is 36 %. In contrast, dip wells on arable  
180 land are underrepresented in the dataset by a factor of 6. The fraction of arable land on  
181 German organic soils is 24 %, and the fraction in the dataset is 4 %. The other two key land  
182 use types on organic soils in Germany, grassland and forest, are well represented in the  
183 dataset. The misbalance of the land use types in the dataset is accounted for in the weighting  
184 of data (see section [2.3.2](#)).

Gelöscht: 2.3.3

186 If land use changed within the measurement period of a dip well, the time series was split at  
187 the moment when the land use record indicates the transition. For each segment the annual  
188 mean water level, WL (here with negative values defined as water levels below ground), was  
189 calculated as multi-year average value over the whole measurement period of the specific land  
190 use.

191 The primary application of the WL map produced in this study is for the upscaling of long-  
192 term GHG emissions as emission reporting may only reflect anthropogenic effects, but no  
193 inter-annual climatic effects. As GHG transfer functions are developed on annual data, their  
194 application requires both the long-term annual mean water level, as well as its inter-annual  
195 variability. Due to the non-linear dependence of GHG emissions on WL, single years with  
196 extreme water levels can strongly influence long-term average GHG fluxes. This study is  
197 focused on the regionalization of the long-term annual mean water levels. For this objective,  
198 model building should be based on long-term water level time series to average out the effect  
199 of weather variation within a complete climatic period (commonly 30 years). The existing  
200 nationally available data on water level time series of organic soils, however, does not  
201 comprise a single time series with complete data coverage over the last 30 years. Due to the  
202 lack of sufficient long-term water level time series, we included all time series in the model  
203 building process. Average climatic boundary conditions (precipitation, reference  
204 evapotranspiration, water balance) of the specific measurement period of each dip well are  
205 part of the predictor variables (see section 2.2), and thus are supposed to partly account for the  
206 effect of specific weather conditions on WL in case of short measurement periods.

## 207 **2.2 Predictor Variables**

208 Spatial coverage of phreatic water level data of organic soils is too low to obtain WL maps by  
209 simple spatial interpolation (Figure 1). Additional spatial data is needed as basis for  
210 regionalization. Ancillary information that covers fully or at least most of the extent of the  
211 final map is necessary as predictor variables. A comprehensive set of variables (numerical and  
212 categorical) with potential indication for the hydrological condition of an organic soil were  
213 determined for each dip well (Figure 2 and Table 1).

214 The predictor variables, which can partly be found also in Finke et al. (2004), can be divided  
215 into seven groups:

**Gelöscht:** This ancillary information does not necessarily need to fully cover the total map extent, as the applied machine learning algorithm in this study (boosted regression trees, see section 2.3) allows for data gaps. However, the contribution to the final model decreases with increasing number of gaps in the predictor variable.

**Feldfunktion geändert**

224 **Land cover:** As certain land use and vegetation requires and reflects certain WL, such  
225 information can be used as indicator for average drainage level around the dip well. Land use  
226 and vegetation information was based on the German Digital Landscape Model (ATKIS  
227 Basis-DLM), which is updated continuously by aerial photos as well as sporadic ground  
228 mapping and has a temporal accuracy of 3 months to 5 years. It is provided as fine-scaled  
229 polygons and represents the best uniform land cover information available in Germany. It  
230 contains information on primary land use type, few optional vegetation attributes and whether  
231 'wet soil' has been observed during mapping. As we noticed that the use of a large number of  
232 categorical variables lowers the performance of boosted regression trees, we further  
233 aggregated the three information types i) land use, ii) vegetation and iii) wet soil into a set of  
234 nine combined land cover classes (Table 1). These land cover classes were a trade-off  
235 between fine differentiation and the number of replicates in each class. For grasslands, a 'wet  
236 grassland' class was separated, when grassland was overlaid with wet soil and/or tree or  
237 shrubs vegetation, which may indicate a less intensive management. Forests overlaid with wet  
238 soil were separated as 'wet forest'. Further, unused peatlands overlaid with wet soil and  
239 showing no coverage with tree attribute were characterized by higher water levels and were  
240 thus separated as 'wet unused peatland'. The very few dip wells classified as open water (n=2)  
241 and peat cutting (n=5) were merged to the reed and arable land cover class, respectively. Land  
242 use type and land cover class were extracted at the dip well (point extraction) and as fractions  
243 in various buffers around the dip well (Table 1). As using too many weak predictor variables  
244 lowers model performance and increases overfitting, the numerous land cover fractions were  
245 further aggregated into two classes: the fraction of dry (arable and grassland) and wet (reed,  
246 wet grassland, wet forest, and wet unused peatland) land cover on organic soils. For the  
247 calculation of the fraction of dry land cover, we tested various factors for the reduction of the  
248 contribution of grassland compared to arable land, as the grassland class also includes wetter  
249 grasslands that could not be detected with the available land cover catalogue. A factor of 0.5  
250 was an optimal value, which was then set fixed.

Gelöscht: , influence of the latter reduced by the factor 0.5

251 **Drainage network:** Locations of ditches that are included as lines in the Digital Landscape  
252 Model were used to obtain information about the drainage network. The total length of  
253 ditches was calculated for various buffer sizes. Further, the distance to the next ditch was  
254 calculated for each dip well. A short distance to the next ditch may indicate either lower or  
255 higher water levels, depending on whether the ditches are used for drainage or already  
256 blocked and used for rewetting measures. Similarly, the indication of total length of ditches is

259 not unique. Therefore, we defined two different sets of ditch variables. A first set, for which  
260 we calculated values for all land cover classes and a second one, for which we only calculated  
261 values for land cover classes for which ditches are undoubtedly used for drainage, i.e. arable  
262 and grassland.

263 **Peatland characteristics:** The geological map of Germany (scale 1:200,000) defined the area  
264 for which WL predictions were modeled. It is also the basis for topological peatland predictor  
265 variables, i.e. the fraction of organic soils in different buffer sizes as well as the dip well  
266 distance to the edge of the peatland. Information about the peatland type and the substrate at  
267 the peat base is presented in more detail in a newly compiled raster map of organic soils  
268 (Roßkopf et al., submitted), and was thus extracted from this map. Peatland types were  
269 aggregated into five classes: Lowland bog (North German Plains and Alpine Forelands),  
270 upland bog (Central Uplands and Alps), fen neighboring surface water, fen without  
271 neighboring surface water, and a class of 'other organic soils' that do not fulfill the C content  
272 and thickness criteria to be classified as peatland. Substrates at the peat base included loose  
273 unconsolidated rock (alluvial sand and gravel deposits), consolidated rock (bedrock) and peat  
274 clay layer. The first type may indicate the occurrence of seepage (positive or negative),  
275 whereas the latter two types may indicate rather a hydraulic decoupling from the aquifer  
276 hydraulic head.

Gelöscht: {Roßkopf, submitted #610}

277 **Climatic boundary conditions:** Climatic boundary conditions directly influence water level.  
278 On the one hand, the typical long-term climatic boundary conditions may indicate the general  
279 vulnerability of peatlands in a specific region. On the other hand, given the different lengths  
280 of measurement periods of the time series in this study, climatic boundary condition predictor  
281 variables may account for the effect of a climatically wetter or drier measurement period,  
282 compared to the long-term averages, on the water level. Climatic boundary conditions were  
283 extracted from a 1x1 km raster of the German Weather Service. Annual, summer and winter  
284 precipitation, FAO56 Penman-Monteith reference evapotranspiration, and climatic water  
285 balance (difference between precipitation and reference evapotranspiration) were determined  
286 for the individual measurement period of each dip well and as long-term averages (30 years).

287 **Relative altitude:** Relative altitude was calculated by subtracting the median altitude of  
288 various buffer sizes from the absolute altitude at each dip well in the DEM. Relative altitude  
289 is expected to have two different indications depending on the applied buffer size: i) In many  
290 peatlands, the former smooth peatland relief at the scale of approximately > 5 m has been

292 disturbed due to peat cutting and differences in drainage and mineralization rate. As a  
293 consequence, the rather smooth phreatic surface often does not follow the uneven and patchy  
294 terrain. Relative altitude with respect to smaller buffer sizes (< 250 m) may therefore explain  
295 part of the WL variation, e.g. a dip well that is located at a surface much higher than the  
296 surrounding may indicate deeper water levels; ii) for large buffer sizes (> 250 m) relative  
297 altitude indicates whether the peatland lies in a larger morphological depression or elevation,  
298 and thus may indicate whether large scale lateral inflow of water can be expected or not.  
299 Similar indication is provided by the topographic index (see below). The accuracy of relative  
300 altitude values depends on the resolution and accuracy of the DEM. The nation-wide available  
301 DEM is based on datasets of varying quality, which may lower the influence of this variable.

302 **Topographic wetness index:** The topographic wetness index is a common wetness indicator  
303 used in hydrology (Beven and Kirby, 1979). It is a combined measure of catchment area and  
304 slope at a given point and indicates the extent of flow accumulation. High values indicate  
305 wetter conditions. If calculated at larger scales, higher values may be a hint for the occurrence  
306 of positive seepage, i.e. upward flow of water from the aquifer. Topographic wetness index,  
307 was calculated for various DEM resolutions using the GRASS 7 module r.watershed.

308 **Protection status:** The protection status of a peatland area may reflect hydrological  
309 conditions. Therefore we checked for seven protection status at each dip well (see Table 1 for  
310 details).

311

### 312 2.3 Model building scheme

313 Model building was performed using boosted regression trees (BRT), implemented in the two  
314 R packages 'gbm' (Ridgeway, 2013) and 'dismo' (Hijmans, 2013). BRT is a machine learning  
315 algorithm, in which the final model is derived from the data. Functions that relate target to  
316 predictor variables are not predetermined but freely developed. BRT is based on the decision  
317 (or regression) tree concept. In the decision tree concept, the parameter space is searched  
318 sequentially for the best split that results into the lowest model mean squared error. The mean  
319 responses of the groups that result from the various splits, and correspond to certain parameter  
320 ranges, represent the model. The common procedure is the growth of a large tree which is  
321 subsequently simplified by dropping weak links that are identified with cross-validation.  
322 Growing only one single tree has several disadvantages like uneven functions that are very

Gelöscht:

Feldfunktion geändert

Gelöscht: It

Feldfunktion geändert

Feldfunktion geändert

Gelöscht: modeling

Formatiert: Englisch (USA)

326 sensitive to the specific sample of the data. Therefore, ensemble techniques have been  
327 combined with the decision tree concept. These were first the development of multiple models  
328 by bootstrapping of the samples (bagging technique) and the random creation of subsets of  
329 predictors at each split (random forest technique). Later, with the 'boosting' technique of BRT,  
330 a sequential procedure was developed in which data is reweighted after each tree to increase  
331 emphasis on data that is poorly modeled by the existing collection of trees (Elith et al., 2008).

Gelöscht: ,

332 BRT modeling is increasingly applied in spatial modeling of species or numerical  
333 environmental variables (Elith et al., 2008, Martin et al., 2011), thereby often showing  
334 superior performance compared to other machine learning algorithms. The increasing  
335 application of BRT is related to several of its favorable characteristics: The strength of this  
336 method lies in the ability to fit complex functional dependencies including non-linear  
337 relationships and interactions between predictor variables. Based on its flexibility, BRT is  
338 invariant to monotonic transformations of predictors. Furthermore, BRT allows for missing  
339 values in the predictor variables, thus predictor variable information does not necessarily need  
340 to fully cover the total map extent. The gbm package handles missing values in predictor  
341 variables by introducing surrogate splits. The mean target value belonging to the missing  
342 predictor values is attributed to these surrogate splits during model building. We observed that  
343 the contribution of a predictor variable to the final model decreases with increasing number of  
344 missing values. This is intuitive, as target observations of missing predictor values are mostly  
345 supposed to scatter strongly. BRT is further fairly insensitive to outliers and allows estimating  
346 the relative contribution of each predictor variable to the model. Due to these characteristics  
347 we expected BRT to be very well suited for the very heterogeneous dataset of this study.

Feldfunktion geändert

Gelöscht: ,

Gelöscht: can estimate

348 BRT model calibration is prone to overfitting, and there are various options to reduce this  
349 behaviour. Due to the overfitting behaviour, cross validation is generally part of the model  
350 building process. However, cross validation can be performed in several ways and, if  
351 performed carelessly, can lead to over-optimistic model performance (De'ath, 2007). Here,  
352 cross validation was performed by leaving out whole peatland areas instead of a random set of  
353 dip wells. This represents a stricter cross validation, and we noticed that it strongly reduced  
354 overfitting of the water level data, and thus contributed to the development of a more robust  
355 model.

Gelöscht: with the major difference that each decision tree has a reduced learning rate. Thus, the final model consists of thousands of overlapping decision trees, similar to the ensemble approach.

Gelöscht: several ways

Feldfunktion geändert

356 Another option to avoid overfitting is to impose monotonic slopes on the effects of individual  
357 parameters, which can even lead to improved prediction performance (De'ath, 2007). For all

Formatiert: Englisch (USA)

Gelöscht: way

Feldfunktion geändert

368 our numerical variables we expected monotonic slopes rather than optimum functions. To  
369 avoid predefining any expected direction, all numerical variables were added twice to the set  
370 of predictors, constraining the slope to a monotonic increase and decrease. We let the model  
371 decide whether monotonic increase or decrease has higher predictive power.

372 Models were calibrated using a Gaussian response type, aimed at minimising deviance  
373 (squared error) (Ridgeway, 2013). In all calibration runs, we applied the `gbm.step` function of  
374 the `dismo` package, which assesses the optimal number of boosting trees using cross  
375 validation. We tested various learning rates (0.001 – 0.01), bag fractions (0.1 – 0.8) and levels  
376 of tree complexity (3 to 7), i.e. the number of nodes in a tree. By trial-and-error we  
377 determined the most effective algorithm parameters for our dataset being 0.005 for the  
378 learning rate, 0.6 for the bag fraction and 5 for the tree complexity.

Feldfunktion geändert

379 The final BRT model building is commonly performed as a two-step procedure (Elith et al.,  
380 2008) which we basically also followed in our study:

Feldfunktion geändert

381 i) In the first step, the whole set of predictor variables is used to calibrate a BRT model.

382 ii) In a second step, the number of parameters is reduced sequentially to avoid overfitting and  
383 to derive a more parsimonious model. We tracked predictive performance criteria during the  
384 simplification process. As various variables were calculated for different buffer sizes, our  
385 predictors included a large number of correlated variables. Correlation coefficients between  
386 predictor variables of  $> 0.7$  are known to severely distort model estimation and subsequent  
387 prediction (Dormann et al., 2013). Thus, we performed this simplification process by first  
388 dropping those parameters with a correlation  $> 0.7$  (either Pearson or Spearman type) to  
389 another parameter with a higher contribution (Clapcott et al., 2011). This avoided that two  
390 highly correlated parameters remain in the parameter set longer than the last parameter of  
391 another group of variables, which may contribute less compared to the two highly correlated  
392 parameters but provides extra information that is not covered by the other parameters. After  
393 all highly-correlated parameters have been dropped, further parameters with low contribution  
394 were dropped progressively.

Feldfunktion geändert

Feldfunktion geändert

395 Predictor contributions are calculated as proportional contributions to the total error reduction,  
396 and can be considered as a measure for the influence of the individual predictors.  
397 Additionally, a BRT model allows to derive partial dependence plots which indicate how the  
398 response is affected by a certain predictor after accounting for the average effects of all other  
399 predictors in the model (Elith et al., 2008). These plots do not show the full effect of each

Feldfunktion geändert

400 parameter on the model response due to interactions with other parameters that are fixed to  
 401 derive these plots as well as due to parameter co-correlation. However, they can be used for  
 402 interpreting model behavior (Elith et al., 2008).

Feldfunktion geändert

403

### 404 2.3.1 $WL_t$ : Transformation of WL

405 The map of water levels of this study was developed to improve the upscaling of greenhouse  
 406 gas emissions from organic soils. Therefore, the final map should provide the highest  
 407 accuracy for the water level range for which the highest differences of greenhouse gas  
 408 emissions occur. This can be achieved by transforming WL into a transformed variable  $WL_t$ ,  
 409 which shows linear relationship with GHG emissions. The sensitivity of greenhouse gas  
 410 emissions to water level has been analyzed in several laboratory and field experimental and  
 411 monitoring studies (Berglund and Berglund, 2011, Drösler et al., 2011, Hahn-Schöfl et al.,  
 412 2011, Leiber-Sauheitl et al., 2014, Moore and Roulet, 1993, Moore and Dalva, 1993, van den  
 413 Akker et al., 2012). General trends are a strong increase of methane ( $CH_4$ ) emissions for  
 414 annual mean water levels of approximately  $> -0.1$  m and an increase of  $CO_2$  emissions for  
 415 water levels  $< -0.1$  m with a trend similar to a saturation function that levels out  
 416 approximately between  $-0.4$  and  $-0.8$  m (Figure 3a). While studies agree over these general  
 417 trends, the exact shape of the transfer function and the maximum levels of emissions as well  
 418 as their dependence on soil properties and other environmental parameters are still discussed  
 419 controversially. Here, we assume a hypothetical transfer function, relating the normalized  
 420 GHG budget, ranging from 0 to 1, to the water level (see also Figure 3),

Gelöscht: (Berglund and Berglund, 2011, Drösler et al., 2011, Hahn-Schöfl et al., 2011, Leiber-Sauheitl et al., 2014, Moore and Dalva, 1993, Moore and Roulet, 1993)

$$421 \quad GHG \text{ Balance} = \begin{cases} -e^{3(WL+0.1)} + 1 & WL \leq -0.1 \\ 1 - e^{-3(WL+0.1)} & WL > -0.1 \end{cases} \quad (1)$$

422 As GHG budget can be positive for both low and high WL, we introduced the transformed  
 423 water level,  $WL_t$ , as (Figure 3),

$$424 \quad WL_t = \begin{cases} e^{3(WL+0.1)} - 1 & WL \leq -0.1 \\ 1 - e^{-3(WL+0.1)} & WL > -0.1 \end{cases} \quad (2)$$

425 By calibrating the model to both WL and  $WL_t$ , we test whether optimization on  $WL_t$  provides  
 426 highest model accuracy for the water level range relevant for GHG emissions and whether it  
 427 optimizes the map for application to GHG upscaling.

432

### 433 2.3.2 Weighting scheme

434 When considering possible data weighting schemes, it is worth emphasizing at this point that  
435 the goal of this study is the development of a statistical model that can explain both the water  
436 level variability within a peatland as wells as among different peatlands. The data on target  
437 and predictor variables for building this model is highly heterogeneous. First, the target  
438 variable dataset contains peatland areas that strongly differ in their spatial extent and in the  
439 number of installed dip wells. Second, the predictor variable dataset contains categorical and  
440 numerical data, and part of the predictor variables predominantly vary from peatland to  
441 peatland (e.g. climatic boundary conditions, large-scale topographic wetness index, peatland  
442 characteristics, ...) whereas others also show within peatland variability (e.g. land use, small-  
443 scale topographic wetness index, drainage network, ...). As the influence of the individual  
444 predictor variables on our target  $WL_t$  is expected being rather diffuse due to abundant  
445 interactions with other site characteristics, the robustness of derived dependencies will  
446 strongly depend on the number of different peatlands in the dataset.

447 There are no universal data weighting rules for similarly heterogeneous data situations and  
448 some degree of expert judgment and subjectivity is inevitable involved when developing an  
449 appropriate scheme (Francis, 2011). ~~The need of introducing a data weighting scheme is~~  
450 obvious, as ~~without data weighting during calibration, too much influence would be~~ given to  
451 small and highly equipped peatlands, which ~~will~~ reduce predictive model performance for  
452 large less well equipped peatland areas. To avoid this in a simple manner, weight could be  
453 reduced by the number of dip wells in each peatland, which results into each peatland being  
454 equally weighted. This scheme however does not sufficiently use the high information content  
455 provided by highly-equipped large peatlands, which should have a higher impact on model  
456 calibration than a small peatland with only few dip wells.

457 Here, we propose a new weighting scheme that takes into account both factors, peatland size  
458 and local density of dip wells, to derive dip well specific weighting factors. It is based on  
459 principles of data uncertainty reduction by repeated measurements and of geostatistics. First,  
460 we consider our data situation as an analogue of meta-analysis with grouped data. It is has  
461 been shown for homogeneous problems (all data from same population) that optimal group  
462 weights for meta-analysis is  $1/SE^2$  (Hedges and Olkin, 1985) with SE being the standard error  
463 of each group.

**Gelöscht:** The dataset contains peatland areas that strongly differ in their spatial extent and in the number of installed dip wells.

**Gelöscht:** To use the information in the data in an optimal fashion, it is important to introduce a weighting of the data. W

**Gelöscht:** is

**Gelöscht:** s

**Gelöscht:** present

**Gelöscht:** n objective

475 
$$SE = \frac{\sigma_e}{\sqrt{N}} \quad (3)$$

476 where  $\sigma_e$  is the error standard deviation of a measurement and N is the number of  
477 measurements in a group. For homogeneous problems and uniform  $\sigma_e$ , this results in weights  
478 that are linearly dependent on N, which we here call the first end member of weighting.  
479 Heterogeneity (within-group variance) reduces the variation of the group weights which can  
480 be shown by random effects models (Cumming, 2012). As second end member of weighting,  
481 when heterogeneity totally dominates within-group variance, optimal group weights are  
482 uniform for all groups, i.e. weights are independent of N. We are not aware of a method that  
483 allows to estimating the degree of heterogeneity for the complex target and predictor data  
484 situation in this study, including data (spatial and temporal variability, measurement error)  
485 and model errors (missing parameters). As a trade-off between 1/SE<sup>2</sup> (homogeneous end  
486 member) and 1 (heterogeneous end member), we decided for a group weight that is the  
487 inverse of the standard error, 1/SE, which is e.g. often used in econometric studies (Dickens,  
488 1990). We emphasize that this is a subjective decision.

489 The group weight, 1/SE, is the basis for the geostatistical part of our weighting scheme. There  
490 are two reasons why we cannot directly treat our peatlands as groups. First, there is within  
491 peatland variability that is related to changing site characteristics. It is one objective of our  
492 study to describe this variability by statistical modeling. Thus, dip wells must be treated  
493 individually and data cannot be aggregated at a peatland level. Second, we expect the model  
494 to learn more when the same number of dip wells is installed in a larger peatland. In a small  
495 peatland, spatial autocorrelation between dip wells is higher, i.e. the information content is  
496 lower than for large peatlands. As a consequence of the first point, we do not aggregate and  
497 keep all dip wells in the target variable dataset by attributing to each dip well the fraction 1/N  
498 of its group weight, so that the relative weights of the groups remain constant. As a  
499 consequence of the second point, we use principles of geostatistics in our weighting scheme.  
500 We replace the group size N (positive integer number) by the 'statistical' group size  $n$  (positive  
501 continuous number being >1), which we derive from the spatial autocorrelation among the dip  
502 wells.

503 Therefore, we analyze the spatial autocorrelation structure of the dataset. A single spherical  
504 variogram model was fitted to the sample variogram of all data (Figure 4 in section 3.1).  
505 Variogram models allow to differentiating the total data variance (called 'sill') into a spatially

Formatiert: Tiefergestellt durch 14 pt

Formatiert: Schriftart: Kursiv

Formatiert: Schriftart: Nicht Kursiv

Formatiert: Schriftart: Kursiv

Gelöscht: ¶

Gelöscht: Dip wells that represent only 'partly repeated' measurements, i.e. indicate some degree of spatial correlation, can be accounted for by

Gelöscht: ing

Gelöscht: Here, we fitted a

Gelöscht: The v

514 uncorrelated variance (called 'nugget') and a spatially correlated variance (called 'structural  
 515 variance' and defined as sill - nugget) (Wackernagel, 2003). The variogram model allows to  
 516 derive for any distance between two locations the average squared difference of values, here  
 517 defined as  $\gamma$ . By definition, at distance 0, the average squared difference equals the nugget,  
 518 and at distances greater than which is called the 'range' of spatial autocorrelation the average  
 519 squared difference equals the sill. Accordingly, the autocorrelated fraction,  $f$ , of the average  
 520 squared difference between two dip wells  $i$  and  $j$  is,

$$521 \quad f_{i,j} = \frac{\text{sill} - \gamma_{i,j}}{\text{sill} - \text{nugget}}. \quad (4)$$

522 We now define the 'statistical' group size,  $n$  of each dip well  $i$  to be the sum of one plus the  
 523 autocorrelated fractions  $f_{i,j}$  of all dip wells that are within the range of spatial autocorrelation  
 524 of  $i$ ,

$$525 \quad n_i = 1 + \sum_{j=1}^m \frac{\text{sill} - \gamma_{i,j}}{\text{sill} - \text{nugget}}. \quad (5)$$

526 According to the discussion above, dip well specific weights can then be calculated with

$$527 \quad w_i = \frac{1}{n_i SE_i} = \frac{1}{\sigma_{e,i} \sqrt{n_i}}. \quad (6)$$

528 where  $n_i$  is derived from Eq. (5). The equation shows that with increasing 'statistical' group  
 529 size  $n$ , i.e. with increasing spatial data density, the weight of an individual dip well is 'down-  
 530 weighted' to some degree, a behavior that corresponds to our initial intention to lower the  
 531 influence of small peatlands compared to large ones. The error standard deviation  $\sigma_e$  is  
 532 dependent on several factors, e.g. the length of the time series, the temporal measurement  
 533 density and the microtopography around the dip well. For simplicity, we here assumed  $\sigma_e$  to  
 534 be uniform for all dip wells, which simplifies Eq. (6) to  $w_i = \frac{1}{\sqrt{n_i}}$ .

535 Only dip wells with the same land use type were summed up with Eq. (5), which avoids the  
 536 down-weighting by dip wells having different land use type. The latter are mostly  
 537 characterized by fairly different WL, thus by rather low spatial autocorrelation to dip well  $i$ .

538 After spatial correlation has been accounted for, the sum of the weights of all dip wells of  
 539 each land use type were adjusted that they correspond to the fractions of this land use type in

Formatiert: Schriftart: Kursiv

Formatiert: Schriftart: Kursiv

Formatiert: Schriftart: Kursiv

Formatiert: Schriftart: Kursiv

Gelöscht: provides a nugget, a sill, and a range of spatial correlation for the given dataset of WL. The fraction of spatial correlation, i.e. the correlated data variance, can now be obtained for any distance between two dip wells  $i$  and  $j$  by:

Gelöscht: 8

Gelöscht: Parameter

Gelöscht: of Eq. (7) can be determined for

Gelöscht: as

Gelöscht: contributions

Formatiert: Schriftart: Kursiv

Formatiert: Tiefgestellt

Gelöscht: :

Gelöscht: 9

Formatiert: Englisch (USA)

Formatiert: Schriftart: Kursiv

Formatiert: Tiefgestellt

Formatiert: Schriftart: Kursiv

Formatiert: Schriftart: Kursiv

Formatiert: Tiefgestellt

Gelöscht: where  $\gamma_j$  is calculated based on the variogram parameters and the distance between dip well  $i$  and  $j$ .

Gelöscht: 9

Gelöscht: of

Gelöscht: with

Formatiert: Tiefgestellt

561 Germany. This adjustment accounts for the overrepresentation in the dataset of dip wells in  
 562 unused peatlands and underrepresentation of dip wells in arable land.

563

564 **2.3.3 Model performance criteria**

565 Model fit and predictive performance after cross-validation were quantified by the weighted  
 566 root mean square error,

567 
$$\text{RMSE} = \sqrt{\frac{1}{\sum_{i=1}^m w_i} \sum_{i=1}^m (w_i (x_{o,i} - x_{s,i})^2)}, \quad (7)$$

568 where  $m$  is the number of dip wells,  $x_{o,i}$  is observed WL or  $WL_t$  of dip well  $i$ ,  $x_{s,i}$  is  
 569 simulated WL or  $WL_t$  of dip well  $i$ , and  $w_i$  is the data weight of dip well  $i$  (see below). We  
 570 refer to the root mean square error of the predicted data of cross validation by  $\text{RMSE}_{cv}$ . Model  
 571 performance was further quantified by Nash-Sutcliffe Efficiency (NSE),

572 
$$\text{NSE} = 1 - \frac{\sum_{i=1}^m w_i (x_{o,i} - x_{s,i})^2}{\sum_{i=1}^m w_i (x_{o,i} - \bar{x}_o)^2}, \quad (8)$$

573 where  $\bar{x}_o$  is the mean of all observed WL or  $WL_t$ . It indicates how well observed vs.  
 574 predicted values match the 1:1 line. NSE is a good overall indicator of predictive performance  
 575 because it combines scatter and bias (common offset and/or slope difference from 1:1 line)  
 576 (Nash and Sutcliffe, 1970). Values greater than 0 signify a model that is better than the  
 577 reference model based on the data mean. We refer to the NSE of the training data by  $\text{NSE}_{cal}$ ,  
 578 and of the predicted data of cross validation by  $\text{NSE}_{cv}$ .

579 Systematic errors were quantified by calculating the model bias, here defined as,

580 
$$\text{BIAS} = \sum_{i=1}^m (w_i x_{o,i} - w_i x_{s,i}) \quad (9)$$

581 **2.4 Model uncertainty and stability evaluation**

582 Uncertainty of the model predictions was assessed by bootstrapping, cross-validation and  
 583 residual analysis.

584 For the bootstrapping analysis, we followed the procedure of Leathwick et al. (2006). We  
 585 estimated the confidence intervals around the predictions and the fitted functions by taking

Gelöscht: 3

Gelöscht: 4

Feldfunktion geändert

Gelöscht: ¶

¶ A common way to introduce individual data weights is to use the inverse of the error variance  $\sigma_e^2$ . For dip well  $i$  the weight is:¶

$$w_i = \frac{1}{\sigma_{e,i}^2} \dots \dots \dots (5)¶$$

Let us consider the extreme case that there are two dip wells separated by only a few meters, so they are basically totally correlated regarding their water level dynamics. The absolute water level, however, may differ between the two dip wells due to micro-topography and measurement error. The second dip well can be considered as a repeated measurement. A reasonable approach would be to take the mean of both measurements and to reduce the error variance by the inverse of the square root of the number of measurements, for this example  $n=2$ , which is common statistics for repeated measurements:¶

$$w_i = \frac{1}{\sqrt{n} \sigma_{e,i}^2} \dots \dots \dots (6)¶$$

Instead of taking the mean of the two dip wells, it is equally possible to keep both dip wells. Then the weight of each dip must be divided by the number of fully-correlated measurements, here  $n=2$ :¶

$$w_i = \frac{1}{n \sqrt{n} \sigma_{e,i}^2} \dots \dots \dots (7)¶$$

Feldfunktion geändert

617 1000 bootstrap samples of the 53 peatlands. The number of peatlands in each sample was  
618 equivalent to the dataset, but peatlands were selected randomly with replacement. Using the  
619 predictor variables of the final model, a BRT model was fitted to each sample. Cross  
620 validation was again performed on peatlands, thus a peatland in the calibration dataset was  
621 not part of the cross-validation dataset to avoid over-optimistic results. Variances of the  
622 predictions and of the fitted functions of the 1000 models were evaluated.

623 If datasets are relatively small (e.g.  $n < 1000$ , (De'ath, 2007)) then the small size of the  
624 training and test datasets lowers model accuracy. Given the fairly small number of peatlands  
625 in the dataset and the partly high spatial correlation of dip wells within these peatlands, we  
626 decided not to split the dataset into a training and test dataset. Estimates of model accuracy  
627 can then be based on cross-validation, thereby making effective use of all the data (De'ath,  
628 2007). The prediction uncertainty of the final model is estimated by the root mean square  
629 error of prediction ( $RMSE_{cv}$ , see above) for each land cover class. After testing for normal-  
630 like distribution of the residuals,  $RMSE_{cv}$  can be used to derive the 68 and 95 % confidence  
631 intervals of the predictions with  $RMSE_{cv}$  and  $2 * RMSE_{cv}$ , respectively.

632 Finally, additional residual analysis was performed to evaluate whether the predictions are  
633 biased for different land cover classes or geographical regions.

634

## 635 **2.5 Regionalization**

636 In the final regionalization step, the predictor variables contributing to the final model were  
637 determined at a 25x25 m raster for all organic soil in Germany. Predictor variables were  
638 determined with the same map input that was used for model building. Land cover  
639 information including information on ditches was based on the data from year 2012 and the  
640 climatic data was based on the average of the last 30 years. The fine spatial resolution of  
641 25x25 m was not chosen to fool the reader with a spatially highly accurate model. But, this  
642 fairly fine scale was necessary to map the relatively small scale effects of the topography,  
643 land use and peatland geometry variables. The final model was then used to make a prediction  
644 for each of these raster cells.

645

Feldfunktion geändert

Feldfunktion geändert

## 646 3 Results and Discussion

### 647 3.1 Spatial correlation structure of the dataset

648 The variogram model fitted to the sample variogram provided a nugget (0.012 m<sup>2</sup>; 0.11 m), a  
649 sill (0.09 m<sup>2</sup>; 0.3 m), and a range of spatial correlation (2700 m) for our dataset of WL (Figure  
650 4). The nugget represents the very small-scale soil hydraulic variability and micro-topography  
651 effects on WL (van der Ploeg et al., 2012) and measurement error, e.g. by differences in the  
652 determination of the ground surface and in the timing of the manual measurements.  
653 Furthermore, micro-topography (e.g. hummocks) and oscillating peat surfaces of wet  
654 peatlands pose a challenge for an accurate determination of both ground surface and water  
655 level. The water level time series in the dataset were of different lengths and ranged from 1 to  
656 20 years. Interannual variability of water levels can be large (e.g., Knotters and van Walsum,  
657 1997). For simplicity, in our analysis, data were not harmonized by extrapolating WL time  
658 series using weather data to a 30-year period. Thus, the nugget also includes errors that are  
659 introduced by dip wells with different measurement periods that are located in the range of  
660 spatial correlation. In consideration of these error sources, the fitted nugget of 0.11 m appears  
661 to be a realistic value. The fitted sill matched with 0.3 m nearly perfectly the standard  
662 deviation of the data (0.31 m), which indicates consistency between semivariogram model  
663 and dataset. The fitted range of spatial correlation of 2700 m reflects both physical effects, i.e.  
664 the average range of lateral flows due to hydraulic gradients, as well as the effect of average  
665 land use patterns in Germany on spatial correlation of WL. Fitted values were used in the  
666 calculation of the dip-well specific weights using Eq. (6).

Feldfunktion geändert

Feldfunktion geändert

Gelöscht: 7

Gelöscht: and (9)

### 667 3.2 Typical water levels for land use types in German organic soils

668 The land cover classes are characterized by plausible mean and median water levels, which  
669 show consistent differences among each other (Table 2 and Figure 5a). The mean values of  
670 arable land and grassland agree with what can be expected for their agronomic requirements,  
671 with slightly lower water levels for arable land. The high variability observed for both classes  
672 may be related to the variability of the efficiency of installed drainage systems, as e.g. the  
673 presence and condition of tile drains and the depth of ditches. Grasslands can be managed  
674 with very variable intensity, which is partly reflected in different water levels. Figure 5a  
675 further shows that deciduous forests seem to dominate on slightly drier organic soils  
676 compared to coniferous forests, which dominate under wetter conditions. A high variability of

679 water levels is observed for the land cover class 'unused peatland'. On the one hand, post peat-  
680 cutting topography increases the variability of WL over short distances. It probably  
681 contributes to the high variance observed for this class. On the other hand, this class  
682 comprises both rather dry unused peatlands and wetter peatlands in which re-wetting  
683 measures already took place, which however do not show yet a 'wet soil' attribute in the  
684 ATKIS Digital Landscape Model. This may also cause part of the variance observed in the  
685 grassland and forest land cover class. All 'wet' land cover classes (reed, wet grassland, wet  
686 forest, and wet unused peatland) that were separated by wetness indication clearly show  
687 higher water levels, showing the wetness attribute of the Digital Landscape Model is a useful  
688 attribute.

689 Figure 5b shows the transformed water level for all classes. It can be observed that the  
690 variances of the wetter land cover classes relatively increase compared to the variances of the  
691 dry land cover classes. This is due to the highest sensitivity of GHG emissions in the wet  
692 range of water levels ( $> -0.5$  m). Consequently, the rather high variance of WL for arable land  
693 corresponds to a rather low variance of  $WL_t$ , i.e. to a rather low assumed effect of WL  
694 variability on the GHG budget.

### 695 **3.3 BRT model calibration and validation: WL vs. $WL_t$**

696 In contrast to land cover class, the other predictor variables showed, if at all, only weak  
697 relations to WL and  $WL_t$  when evaluating them with box plots, 2D cross plots and simple  
698 correlation matrices. Here, we expected BRT to detect the strongest predictor interactions and  
699 to identify the most informative predictors.

700 After model calibration with all predictors, subsequent model simplification successively  
701 dropped those parameters with correlation  $> 0.7$  and lowest contribution. For both, WL and  
702  $WL_t$ , model performance improved during this simplification. For  $WL_t$ , highest values of  
703  $NSE_{cv}$  of approximately 0.46 were achieved with 21 to 9 model parameters. The development  
704 of  $NSE_{cv}$  for the last 50 parameters is shown in Figure 6. Further elimination of parameters  
705 led to a pronounced decline of model performance. Similar behavior was observed for the  
706 calibration on WL. In favour of a more parsimonious model we chose the model with the  
707 lowest number of parameters before the pronounced decline of model performance occurred.  
708 For the calibration on  $WL_t$ , this corresponded to the model with lowest number of parameters  
709 that still achieved  $NSE_{cv}$  values of  $> 0.45$  (Figure 6). The final  $WL_t$  model comprised nine

710 predictor variables, and the final WL model seven parameters. The percentages of parameter  
711 contributions to the final model and their individual influences are discussed for  $WL_t$  in  
712 section 3.4.

713 Table 3 summarizes the statistical performances of the models calibrated on WL and  $WL_t$ . For  
714 both models  $NSE_{cal}$  is considerably higher than  $NSE_{cv}$  and shows the commonly observed  
715 overfitting behavior of BRT models. The different measures that we conducted to minimize  
716 overfitting (cross-validation on peatlands, restriction to monotonic responses, and model  
717 simplification including elimination of highly correlated variables) lowered the difference  
718 between  $NSE_{cal}$  and  $NSE_{cv}$  but could not totally avoid overfitting.  $NSE_{cv}$  of the  $WL_t$  model  
719 (0.453) indicates higher predictive model performance compared to the WL model (0.381).  
720 However, as the data ranges differ due to the transformation, this comparison may be  
721 misleading. Therefore, we transformed the predictions of the WL model to obtain  $WL_t$  values  
722 from this model and equally calculated the performance criteria (Table 3, second column).  
723 Then,  $NSE_{cv}$  is slightly increased (0.397), but does not achieve the values of the model that  
724 was calibrated on  $WL_t$ . A better predictive model performance of the model calibrated on  $WL_t$   
725 is also visible for the  $RMSE_{cv}$  values. The total  $RMSE_{cv}$ , as well as the  $RMSE_{cv}$  values for the  
726 dry ( $WL < -0.3$  m) and wet range ( $WL > -0.3$  m), show slightly lower values for the  $WL_t$  model  
727 compared to  $WL_t$  values from the model calibrated on WL. Given our hypothetical transfer  
728 function (Figure 3) in which the GHG budget is linearly related to  $WL_t$ , the higher accuracy  
729 of  $WL_t$  predictions directly corresponds to a higher accuracy of GHG budget predictions.

730 Superior model performance is also evident when evaluating model bias. Only when  
731 calibrating directly on  $WL_t$ , the  $WL_t$  predictions are bias-free. Calibration on WL and  
732 subsequent transformation to  $WL_t$ , introduces a model bias towards systematically lower  $WL_t$   
733 values. In subsequent applications to GHG emission upscaling, lower  $WL_t$  values would lead  
734 to an overestimation of  $CO_2$  emissions and to an underestimation of  $CH_4$  emissions.

### 735 **3.4 Influence of predictor variables on $WL_t$**

736 Given the beneficial characteristics of the model calibrated on  $WL_t$  for GHG upscaling,  
737 presentation and discussion of further model results is restricted to the  $WL_t$  model.

738 The BRT method allows to analyze the parameter contributions to and influences on the  
739 model (Elith et al., 2008) and thus may contribute to the system understanding. The  
740 percentages of the contributions of the nine predictor variables to the final model ranged from

Feldfunktion geändert

741 25.2 % to 5.6 % (Figure 7). Except of protection status, at least one parameter of each of the  
742 seven parameter groups contributed to the final model. All protection status information was  
743 dropped early during the simplification process due to low contribution, although WL showed  
744 slightly higher values for data from Nature Protection or Special Areas of Conservation.  
745 However, other parameters seem to be able to fully compensate the information that is lost by  
746 dropping this predictor.

747 Land cover class, lc, at the dip well was the parameter with strongest contribution (25.2 %). It  
748 basically follows the trend illustrated in Figure 5b. The bootstrap error plotted as standard  
749 deviation (Figure 7) shows the variation of this influence over the 1000 bootstrap models. A  
750 second land cover parameter, the fraction of dry land cover classes on organic soils in a buffer  
751 of 2500 m radius,  $f_{dry}(2500)$ , contributed to the model with 10.3 %. The monotonic decrease  
752 of  $WL_t$  with increasing  $f_{dry}(2500)$  is plausible, as higher values reflect intensive land use in the  
753 surroundings of the dip well and thus indicate intensive artificial drainage. Together both  
754 parameter contributed by 35.5 % and thus land cover represents the parameter group with the  
755 strongest model contribution.

756 Peatland characteristics are the second most important parameter group. The peatland type  
757 contributed by 16 %. The model indicates that peatlands without any connection to surface  
758 water bodies (river or lake) and the class of other organic soils are characterized by lower  $WL_t$   
759 compared to the peatland types lowland bog, upland bog and fen neighboring surface water.  
760 As the class of other organic soils is generally expected to reflect lower water levels and as  
761 surface water may have a stabilization effect on water levels of organic soils, the influence of  
762 the peatland type can be considered as plausible. Besides peatland type, the substrate of the  
763 peat base contributes by 5.6 %. Here, organic soils overlying peat clay layers (e.g. limnic  
764 sediments like calcareous gyttja) or basement rock are characterized by higher  $WL_t$  compared  
765 to organic soils overlying unconsolidated rock. This can be explained by the lower drainage  
766 resistance of unconsolidated rocks. This may cause an increased efficiency of anthropogenic  
767 drainage and/or a general higher vulnerability to seepage losses. Finally, slightly lower  $WL_t$   
768 values are indicated by a high fraction of organic soils for the 500 m buffer,  $f_{peat}(500)$ . This  
769 may reflect the higher land use pressure on large peatlands compared to rather small  
770 peatlands, which tentatively are more easily preserved by nature protection efforts.

771 The remaining four parameter groups are represented in the model by only one parameter  
772 each. The third most influential parameter was the length of ditches on arable land and

Gelöscht: limnic sediments

774 grassland for the 250 m buffer,  $di_{\text{en,dry}}(250)$ . At first glance, it may be surprising that with  
775 increasing ditch density,  $WL_t$  values tend to be higher, as ditches are supposed to drain the  
776 water when land is used as arable land and grassland. The fact that the model identifies a  
777 rather strong effect in the opposite direction may be caused by the incomplete information  
778 about the drainage network. There is not detailed information about the spatial distribution of  
779 tile drains. Based on expert knowledge, agricultural areas with a lower ditch density are more  
780 likely to be equipped with tile drains. As the latter, easily installed with a narrow drain  
781 spacing, are more effectively draining organic soils, low  $WL_t$  values for arable land and  
782 grassland may be related to low ditch densities. Furthermore, ditches were originally dug at  
783 narrow spacing in especially wet areas of organic soils, but there is no information available  
784 whether these ditches still function properly.

785 The parameters  $wb_{\text{summer}}$ ,  $h_{\text{rel}}$  and  $ti_{\text{ras25}}$  all show expected trends. The model predicts higher  
786  $WL_t$  for increasing climatic water balance in the summer period (May to October),  $wb_{\text{summer}}$ ,  
787 and for dip wells located in depressions (low values of  $h_{\text{rel}}$ ), and for higher small-scale  
788 topographic wetness indices calculated on the 25x25 digital elevation model ( $ti_{\text{ras25}}$ ).

789 The fact that all parameters show expected or explainable responses in the model corroborates  
790 the reliability of the calibrated  $WL_t$  model. The standard deviation of the predictor responses  
791 based on the bootstrap samples shows the stability of the observed responses.

792 Further insights into model behavior can be obtained by analyzing parameter interactions.  
793 This is obtained by changing two parameters simultaneously while keeping mean values for  
794 all other parameters (Elith et al., 2008). Figure 8 shows the two strongest parameter  
795 interactions. Parameter  $wb_{\text{summer}}$  strongly interacts with  $p_{\text{type}}$ . The generally lower values of  
796  $WL_t$  of fens without surface water connection and other organic soils show a stronger  
797 dependency on the summer climatic water balance. While a summer climatic water balance of  
798  $> -80$  mm shows rather low further effect on  $WL_t$  for the wetter peatland types, in contrast for  
799 the two drier peatland types there is still a strong effect with increasing  $wb_{\text{summer}}$ . The trend for  
800  $wb_{\text{summer}} > 130$  mm for the dry peatland types is supported by seven different peatlands.

801 Another strong interaction is observed for  $p_{\text{base}}$  and  $f_{\text{dry}}(2500)$ . While a rather low effect of the  
802 fraction of arable land and grassland is observed for organic soils overlying basement rock  
803 and peat clay layer, strong effect is observed for organic soils overlying unconsolidated rock.  
804 This interaction reflects the higher lateral range of drainage effects for organic soils with little

Feldfunktion geändert

805 flow resistance at the peat base. In these organic soils, intensive land use lowers water level  
806 over large areas.

### 807 **3.5 Discussion of model uncertainty**

808 Plotting observed vs. predicted  $WL_t$  from cross-validation (Figure 9) illustrates the rather  
809 large residual variance that cannot be explained by the model. As indicated by the higher  
810  $RMSE_{cv}$  for the wet range (Table 3), scatter increases with increasing  $WL_t$ . Error bars in the  
811 y-direction indicate data error derived from the nugget of the variogram. It is exemplarily  
812 shown for a few data points. Due to transformation, data error increases for higher  $WL_t$ .  
813 Figure 9 demonstrates that the fraction of unexplainable variance related to data error is much  
814 higher for the wet than for the dry range. Bootstrap error that indicates the variation of the  
815 model predictions for 1000 bootstrap samples is shown in the x-direction for the same data  
816 points. Bootstrap error is lower than the data error for the wet range and slightly higher for the  
817 dry range.

818 Bootstrap errors demonstrate the sensitivity of model predictions to changes of the dataset  
819 used for calibration. When a model possesses structural deficits, such as missing predictor  
820 variables, bootstrap errors should not be used to define confidence intervals for the model  
821 predictions. Figure 10 shows residuals from cross-validation and standard deviation of  
822 bootstrap predictions for all land cover classes. The residuals of each land cover class show  
823 normal-like distributions. For five of the nine land cover classes (wet forest, wet unused  
824 peatland, arable land, coniferous forest, and reed), Shapiro-Wilk test of normality is positive  
825 ( $p > 0.05$ ). Figure 10a further indicates that residuals of each land cover fairly well scatter  
826 around zero, indicating low bias for the various land cover classes. Land cover class specific  
827 confidence intervals of model predictions can thus be derived from the  $RMSE_{cv}$  of each land  
828 cover class, e.g.  $2 * RMSE_{cv}$  representing the 95% confidence interval.

829 The prediction uncertainty derived from cross-validation is much higher than the bootstrap  
830 prediction uncertainty obtained from the bootstrap standard deviation (sd), with  $2 * sd$   
831 corresponding to the 95% confidence interval (Figure 10). The large difference between these  
832 values indicates that the model has structural deficits that can be attributed to several error  
833 sources:

834 i) Key influences on  $WL_t$  are missing in the set of predictor variables. None of the predictor  
835 variables indicate whether and to which extent water level increase due to re-wetting

836 measures took place in the last years. Wetness indicators (wet soil and/or vegetation  
837 attributes) that are obtained from the Digital Landscape Model probably react with a delay of  
838 several years. Thus, we expect the occurrence of several observed high  $WL_t$  values that  
839 cannot be explained by any of the predictor variables.

840 ii) Small-scale topography that is not represented with sufficient detail and accuracy in the  
841 DEM may cause that several predictions strongly differ from what would be expected from  
842 the other predictor variables. A common example may be a dip well that is located on a  
843 narrow peat ridge, which remained after peat-cutting and is absent in the DEM, and that is  
844 situated in an area classified as wet soil by the Digital Landscape Model. Then, the model  
845 indicates a  $WL_t$  that is much higher than the observed  $WL_t$ , as for the observed value the  
846 reference surface was the surface of the peat ridge.

847 iii) Consistent information about tile drains is missing and only exists regionally (Tetzlaff et  
848 al., 2009). At the national scale, however, there are no maps on tile drains. Tile drains are  
849 known to have a strong effect on  $WL_t$  for arable land and grassland. As explained above, we  
850 expect parameter  $di_{len,dry}(250)$  to partially compensate for this missing information.

851 iv) Another source of prediction uncertainty may comprise inconsistent and erroneous land  
852 cover classification of the Digital Landscape Model due to the high degree of subjectivity for  
853 many of the attributes. Furthermore, the temporal accuracy of the Digital Landscape Model  
854 may be as bad as 5 years which can cause time series with land use change to be split at the  
855 wrong date, and vegetation and wetness attributes not yet to be updated to the current  
856 conditions.

857 v) The water balance of fens strongly depends on the size and the hydraulic head of the  
858 groundwater catchment, **i.e. of the aquifer underlying the peat layer**. Unfortunately, there is no  
859 consistent map on hydraulic heads or groundwater catchments for all Germany.

860 We checked model predictions for geographical bias. Geographical location was not one of  
861 the model parameters. However, history and policy of land use on organic soils, current ditch  
862 water management and climate do show large-scale geographical trends. We divided our  
863 dataset into the three major German peatland regions (NE, NW and S) and evaluated the  
864 model residuals (Figure 11) to see whether our model is biased due to important missing  
865 geographical effects. A serious bias for any of the three major German peatland regions  
866 cannot be identified.

Feldfunktion geändert

867 When applying calibrated statistical models during regionalization, it is important to check  
868 model behavior for extrapolation outside the range of the parameter space that is covered by  
869 the data upon which the model was built. BRT always extrapolates at a constant value from  
870 the most extreme environmental value in the training data. In contrast to other types of  
871 statistical models, e.g. generalized linear models, BRT does not continue the fitted trend  
872 beyond the last observation. Regarding the categorical variables, the dataset covers all classes  
873 occurring in Germany with several peatlands. The dataset also covers the major range of  
874 values occurring in Germany for the numerical predictor variables. Furthermore, Figure 7  
875 indicates that the constant values, at which the model extrapolates the influence of the  
876 variables, do not raise major concern for any extreme predictions outside the parameter range.

### 877 **3.6 Regionalization**

878 The map of  $WL_t$  resulting from the application of the fitted  $WL_t$  model to all grid cells shows  
879 gradients at the regional scale (Figure 12a). E.g., in the south of Germany, a gradient from  
880 wet to dry can be observed for the pre-alpine upland bogs and the peatlands of the moraine  
881 plain. In the north of Germany, the map indicates that organic soils in the very NE are wetter  
882 than the rest. For the rest of the north a slight gradient can be observed from less dry to dry  
883 from NW to E, which is mainly driven by the higher summer climatic water balance in the  
884 NW. As both categorical and numerical predictor variables do also vary at sub-regional scale,  
885 the resulting map also shows gradients within peatland areas, e.g. due to small-scale land use  
886 ditch density gradients and topography effects (Figure 12b).

887 We calculated  $WL_t$  averages of the land cover classes using the regionalized  $WL_t$  from the  
888 map (Table 2, column 3). The given standard deviation comprises both the variability within a  
889 land cover class that is explained by the model as well as the uncertainty of each prediction.  
890 Resulting means and standard deviations slightly differ from the corresponding values of the  
891 dataset. The land cover specific  $WL_t$  values obtained from the map can be considered as being  
892 more representative, as the regionalization procedure is supposed to partly account for  
893 potential bias in the dataset.

894 When applying this map and its predicted  $WL_t$  values in subsequent GHG upscaling, it is  
895 crucial that model uncertainty is propagated properly. An example demonstrates the necessity  
896 of uncertainty propagation. For a grid cell classified as wet grassland, the probability  
897 distribution of  $WL_t$  is shown based on a normal distribution that was fitted to the residuals of

898 this land cover class (Figure 12c). Without propagating the uncertainty and when only  
899 translating the predicted  $WL_t$  (eventually in combination with other parameters, e.g. soil  
900 properties) into a GHG budget, GHG budget is strongly underestimated as the  $WL_t$  prediction  
901 is close to zero, indicating neither large  $CO_2$  nor  $CH_4$  emissions. When translating the full  
902 distribution of  $WL_t$  into a GHG budget, the resulting GHG budget would be much higher, as  
903 at both sides of the predicted  $WL_t$  the GHG budget increases.

### 904 **3.7 Possible paths for model improvement**

905 The model performance that is achieved by the statistical approach presented in our study  
906 raises the question whether collecting more WL data can improve model performance or  
907 whether the factor that is constraining the model performance is the limited strength of the  
908 nation-wide available predictor variables. To assess this question, additional ‘holdout models’  
909 were developed by fitting the BRT model to various random sets of data with a limited  
910 number of peatland areas (from 10 to 50 peatlands). For each number of peatland areas, 500  
911 random selections were calibrated and model performance was evaluated with  $NSE_{cv}$ . As  
912 expected, results indicate an increase of model performance with increasing number of  
913 peatlands used in the model building process (Figure 13). Results also indicate a substantial  
914 flattening of the learning curve. Thus, further collection of WL data may only lead to a  
915 substantial model improvement when including many more peatlands into the dataset. More  
916 promising would be the specific collection of more data on the weakly represented and/or  
917 important land cover classes arable land and grassland.

918 Another path to achieve a stronger model improvement is the development of new predictor  
919 variables. In future, the availability of a more accurate DEM based on laser-scanning data,  
920 which is already available at full coverage for some federal states of Germany, may strongly  
921 increase the predictability of the observed WL data. Additionally, a nation-wide map on water  
922 management and on the distribution of tile drains may represent great potential to explain  
923 large parts of the residual variance and/or even allow setting up a large scale physically-based  
924 model that includes water management. Furthermore, data harmonization by extrapolating the  
925 water level time series of our dataset with the climatic boundary conditions of the last 30  
926 years may lower the unexplainable variance of the dataset due to short measurement periods  
927 (Bartholomeus et al., 2008), an effort that has been successfully conducted in Finke et al.  
928 (2004) using the transfer noise model of Bierkens et al. (1999). Finally, we believe that the  
929 inclusion of remote sensing products in our statistical model approach, as e.g. spaceborne

Feldfunktion geändert

Feldfunktion geändert

Feldfunktion geändert

930 microwave soil moisture observations (Sutanudjaja et al., 2013), may hold large potential to  
931 improve model performance as moisture differences due to varying water levels are high for  
932 organic soils.

933

#### 934 **4 Conclusions**

935 Our study demonstrates the potential of statistical modeling for the regionalization of water  
936 levels in organic soils when data covers only a small fraction of peatlands of the final map  
937 and thus spatial interpolation is not possible. With the available dataset of target and predictor  
938 variables, it was possible to predict 45 % of the GHG relevant water level variance in the  
939 dataset in a cross-validation scheme. The variance is explained by nine predictor variables.  
940 With the analysis of their effect on the water level it was possible to gain insights into natural  
941 and anthropogenic boundary conditions that control water levels of organic soils in Germany.

942 Based on a hypothetical GHG transfer function relating GHG emissions to annual mean water  
943 levels (WL) we showed the advantage of transforming the annual mean water level into a new  
944 variable ( $WL_t$ ) to which GHG emissions linearly depend on. The transformation improved  
945 model accuracy, increased the explained variance of the water level range that is relevant for  
946 GHG emissions and avoided model bias.

947 The presented approach is transparent and allows successive improvement when new input  
948 data and predictor variables become available. Our results show that model improvement by  
949 increasing number of  $WL_t$  data, however, seems to be limited. If efforts are made, data  
950 collection should be concentrated in agriculturally used organic soils, for which relatively few  
951 data is available. We believe that the constraining factor of model performance is rather the  
952 weakness of the predictor variables that are currently available at large scales. The  
953 development of new more informative predictor variables, as e.g. water management maps  
954 and remote sensing products, may represent the more promising path for model improvement.

955 The proposed regionalization approach is suited to application to any other country when  
956 similar data on target and predictor variables is available. It is important that the spatial  
957 resolution of the predictor variables is high enough (Finke et al., 2004). If predictor variables  
958 like land use and peatland type are only available at a much coarser scale and provided as  
959 percentages for grid cells, the dependency between predictor variables and the rather local  
960 WL will be probably lost for most of the predictor variables.

Feldfunktion geändert

Feldfunktion geändert

961 Our work must be considered as one piece of a broader framework for the regionalization of  
962 GHG emissions that includes other site characteristics and must be further developed in future  
963 research. For example, if for specific regions detailed information on peat properties becomes  
964 available and its effect on GHG emissions can be estimated by the use of multivariate transfer  
965 functions, the map of transformed water levels (WL<sub>t</sub>) can be used as an input for this follow-  
966 up regionalization.

Formatiert: Tiefgestellt

967

## 968 **Acknowledgements**

969 Several institutions made their data available for this synthesis study. We gratefully thank  
970 ARGE Schwäbisches Donaumoos, Biologische Station Steinfurt, Biosphärenreservat  
971 Vessertal, BUND Diepholzer Moorniederung, Deutscher Wetterdienst (DWD),  
972 Bezirksregierung Detmold, Förderverein Feldberg-Uckermärkische Seenlandschaft,  
973 Hochschule für Wirtschaft und Umwelt Nürtingen (Institut für Angewandte Forschung),  
974 Hochschule Weihenstephan-Triesdorf (Professur für Vegetationsökologie), Humboldt  
975 Universität zu Berlin (Fachgebiet Bodenkunde und Standortlehre), Landkreis Gifhorn, LBEG  
976 Hannover (Referat Boden- und Grundwassermonitoring), LUNG Mecklenburg-Vorpommern,  
977 Dr. Eberhard Gärtner, IGB Berlin (Zentrales Chemielabor), Landkreis Gifhorn, NABU  
978 Minden-Lübbecke, Naturpark Drömling, Naturpark Erzgebirge/Vogtland, Region Hannover,  
979 Naturpark Nossentiner/Schwinzer Heide, Naturschutzfond Brandenburg, Ökologische Station  
980 Steinhuder Meer, Technische Universität München (Lehrstuhl für Vegetationsökologie),  
981 Universität Hohenheim (Institut für Bodenkunde und Standortlehre), Johannes Gutenberg-  
982 Universität Mainz (Geographisches Institut, Bodenkunde), Universität Rostock (Professur für  
983 Bodenphysik und Ressourcenschutz, Professur für Landschaftsökologie und Standortkunde,  
984 Professur für Hydrologie), Kees Vegelin, ZALF (Institut für Bodenlandschaftsforschung,  
985 Institut für Landschaftsbiogeochemie), Dr. Werner Kutsch, Dr. Christian Brümmer, und  
986 Miriam Hurkuck. Furthermore, we acknowledge Maik Hunziger and Sören Gebbert for field  
987 and GRASS support, Katharina Leiber-Sauheitl, Stefan Frank, Ullrich Dettmann and René  
988 Dechow for data processing support, and Dr. Annette Freibauer for reviewing the paper draft.  
989 The study was financially supported by the joint research project “Organic soils” funded by  
990 the Thünen Institute.

991

992 **References**

993

994 [Bartholomeus, R., Witte, J. P. M., van Bodegom, P. M. and Aerts, R.: The need of data](#)  
995 [harmonization to derive robust empirical relationships between soil conditions and vegetation,](#)  
996 [J. Veg. Sci., 19, 799-808, doi:10.3170/2008-8-18450, 2008.](#)

997 [Berglund, O. and Berglund, K.: Influence of water table level and soil properties on emissions](#)  
998 [of greenhouse gases from cultivated peat soil, Soil Biol. Biochem., 43, 5, 923-931,](#)  
999 [doi:10.1016/j.soilbio.2011.01.002, 2011.](#)

1000 [Beven, K. J. and Kirby, M.: A physically based variable contributing area model of catchment](#)  
1001 [hydrology, Hydrol. Sci. Bull., 24, 43-69, 1979.](#)

1002 [Bierkens, M. F. P. and Stroet, C. B. M. T.: Modelling non-linear water table dynamics and](#)  
1003 [specific discharge through landscape analysis, J. Hydrol., 332, 3-4, 412-426,](#)  
1004 [doi:10.1016/j.jhydrol.2006.07.011, 2007.](#)

1005 [Bierkens, M. F. P., Knotters, M. and van Geer, F. C.: Calibration of transfer function-noise](#)  
1006 [models to sparsely or irregularly observed time series, Water Resour. Res., 35, 6, 1741-1750,](#)  
1007 [doi:10.1029/1999wr900083, 1999.](#)

1008 [Buchanan, S. and Triantafilis, J.: Mapping Water Table Depth Using Geophysical and](#)  
1009 [Environmental Variables, Groundwater, 47, 1, 80-96, doi:10.1111/j.1745-6584.2008.00490.x,](#)  
1010 [2009.](#)

1011 [Clapcott, J., Young, R., Goodwin, E., Leathwick, J. and Kelly, D.: Relationships between](#)  
1012 [multiple land-use pressures and individual and combined indicators of stream ecological](#)  
1013 [integrity, Department of Conservation, DOC Research and Development series 326,](#)  
1014 [Wellington, New Zealand, 2011.](#)

1015 [Cumming, G.: Understanding The New Statistics, Routledge, New York, USA, 535 pp., 2012.](#)

1016 [De'ath, G.: Boosted trees for ecological modeling and prediction, Ecology, 88, 1, 243-251,](#)  
1017 [doi:10.1890/0012-9658\(2007\)88\[243:Btfema\]2.0.Co;2, 2007.](#)

1018 [Dickens, W. T.: Error components in grouped data: Is it ever worth weighting?, The Review](#)  
1019 [of Economics and Statistics, 72, 2, 328-333, 1990.](#)

Formatiert: Einzug: Links: 0 cm,  
Erste Zeile: 0 cm

1020 [Dormann, C. F., Elith, J., Bacher, S., Buchmann, C., Carl, G., Carre, G., Marquez, J. R. G.,](#)  
1021 [Gruber, B., Lafourcade, B., Leitao, P. J., Munkemuller, T., McClean, C., Osborne, P. E.,](#)  
1022 [Reineking, B., Schroder, B., Skidmore, A. K., Zurell, D. and Lautenbach, S.: Collinearity: a](#)  
1023 [review of methods to deal with it and a simulation study evaluating their performance,](#)  
1024 [Ecography, 36, 1, 27-46, doi:10.1111/j.1600-0587.2012.07348.x, 2013.](#)

1025 [Drösler, M., Freibauer, A., Adelman, W., Augustin, J., Bergmann, L., Beyer, C., Chojnicki,](#)  
1026 [B., Förster, C., Giebels, M., Görlitz, S., Höper, H., Kantelhardt, J., Liebersbach, H., Hahn-](#)  
1027 [Schöfl, M., Minke, M., Petschow, U., Pfadenhauer, J., Schaller, L., Schägner, P., Sommer,](#)  
1028 [M., Thuille, A. and Wehrhan, M.: Klimaschutz durch Moorschutz in der Praxis, Ergebnisse](#)  
1029 [aus dem BMBF-Verbundprojekt „Klimaschutz - Moornutzungsstrategien“ 2006-2010, vTI-](#)  
1030 [Arbeitsberichte 4/2011, 2011.](#)

1031 [Elith, J., Leathwick, J. R. and Hastie, T.: A working guide to boosted regression trees, J.](#)  
1032 [Anim. Ecol., 77, 4, 802-813, doi:10.1111/j.1365-2656.2008.01390.x, 2008.](#)

1033 [Fan, Y. and Miguez-Macho, G.: A simple hydrologic framework for simulating wetlands in](#)  
1034 [climate and earth system models, Clim. Dynam., 37, 1-2, 253-278, doi:10.1007/s00382-010-](#)  
1035 [0829-8, 2011.](#)

1036 [Finke, P. A., Brus, D. J., Bierkens, M. F. P., Hoogland, T., Knotters, M. and de Vries, F.:](#)  
1037 [Mapping groundwater dynamics using multiple sources of exhaustive high resolution data,](#)  
1038 [Geoderma, 123, 1-2, 23-39, doi:10.1016/j.geoderma.2004.01.025, 2004.](#)

1039 [Francis, R. I. C. C.: Data weighting in statistical fisheries stock assessment models, Can J](#)  
1040 [Fish Aquat Sci, 68, 6, 1124-1138, doi:10.1139/F2011-025, 2011.](#)

1041 [Gong, J. N., Wang, K. Y., Kellomaki, S., Zhang, C., Martikainen, P. J. and Shurpali, N.:](#)  
1042 [Modeling water table changes in boreal peatlands of Finland under changing climate](#)  
1043 [conditions, Ecol. Model., 244, 65-78, doi:10.1016/j.ecolmodel.2012.06.031, 2012.](#)

1044 [Hahn-Schöfl, M., Zak, D., Minke, M., Gelbrecht, J., Augustin, J. and Freibauer, A.: Organic](#)  
1045 [sediment formed during inundation of a degraded fen grassland emits large fluxes of CH<sub>4</sub> and](#)  
1046 [CO<sub>2</sub>, Biogeosciences, 8, 6, 1539-1550, doi:10.5194/bg-8-1539-2011, 2011.](#)

1047 [Hedges, L. V. and Olkin, I.: Statistical Methods for Meta-Analysis, Academic Press, Orlando,](#)  
1048 [USA, 369 pp., 1985.](#)

1049 [Hijmans, R. J.: Species distribution modeling. Documentation on the R Package 'dismo',](#)  
1050 [version 0.9-3, http://cran.r-project.org/web/packages/dismo/dismo.pdf, accessed February](#)  
1051 [2014, 2013.](#)

1052 [Hoogland, T., Heuvelink, G. B. M. and Knotters, M.: Mapping Water-Table Depths Over](#)  
1053 [Time to Assess Desiccation of Groundwater-Dependent Ecosystems in the Netherlands,](#)  
1054 [Wetlands, 30, 1, 137-147, doi:10.1007/s13157-009-0011-4, 2010.](#)

1055 [IPCC: IPCC guidelines for national greenhouse gas inventories, In: Eggleston, H.S., Buendia,](#)  
1056 [L., Miwa, K., Ngara, T., K., T. \(Eds.\). IGES, Japan, 2006.](#)

1057 [Ju, W. M., Chen, J. M., Black, T. A., Barr, A. G., Mccaughey, H. and Roulet, N. T.:](#)  
1058 [Hydrological effects on carbon cycles of Canada's forests and wetlands, Tellus B, 58, 1, 16-](#)  
1059 [30, doi:10.1111/j.1600-0889.2005.00168.x, 2006.](#)

1060 [Knotters, M. and van Walsum, P. E. V.: Estimating fluctuation quantities from time series of](#)  
1061 [water-table depths using models with a stochastic component, J. Hydrol., 197, 1-4, 25-46,](#)  
1062 [doi:10.1016/S0022-1694\(96\)03278-7, 1997.](#)

1063 [Leathwick, J. R., Elith, J., Francis, M. P., Hastie, T. and Taylor, P.: Variation in demersal fish](#)  
1064 [species richness in the oceans surrounding New Zealand: an analysis using boosted regression](#)  
1065 [trees, Mar. Ecol. Prog. Ser., 321, 267-281, doi:10.3354/Meps321267, 2006.](#)

1066 [Leiber-Sauheitl, K., Fuß, R., Voigt, C. and Freibauer, A.: High CO2 fluxes from grassland on](#)  
1067 [histic Gleysol along soil carbon and drainage gradients, Biogeosciences, 11, 735-747,](#)  
1068 [doi:10.5194/bg-11-749-2014, 2014.](#)

1069 [Levy, P. E., Burden, A., Cooper, M. D. A., Dinsmore, K. J., Drewer, J., Evans, C., Fowler, D.,](#)  
1070 [Gaiawyn, J., Gray, A., Jones, S. K., Jones, T., Mcnamara, N. P., Mills, R., Ostle, N.,](#)  
1071 [Sheppard, L. J., Skiba, U., Sowerby, A., Ward, S. E. and Zielinski, P.: Methane emissions](#)  
1072 [from soils: synthesis and analysis of a large UK data set, Global change biology, 18, 5, 1657-](#)  
1073 [1669, doi:10.1111/j.1365-2486.2011.02616.x, 2012.](#)

1074 [Limpens, J., Berendse, F., Blodau, C., Canadell, J. G., Freeman, C., Holden, J., Roulet, N.,](#)  
1075 [Rydin, H. and Schaepman-Strub, G.: Peatlands and the carbon cycle: from local processes to](#)  
1076 [global implications - a synthesis, Biogeosciences, 5, 5, 1475-1491, doi:10.5194/bg-5-1475-](#)  
1077 [2008, 2008.](#)

1078 [Martin, M. P., Wattenbach, M., Smith, P., Meersmans, J., Jolivet, C., Boulonne, L. and](#)  
1079 [Arrouays, D.: Spatial distribution of soil organic carbon stocks in France, \*Biogeosciences\*, 8,](#)  
1080 [5, 1053-1065, doi:10.5194/bg-8-1053-2011, 2011.](#)

1081 [Melton, J. R., Wania, R., Hodson, E. L., Poulter, B., Ringeval, B., Spahni, R., Bohn, T., Avis,](#)  
1082 [C. A., Beerling, D. J., Chen, G., Eliseev, A. V., Denisov, S. N., Hopcroft, P. O., Lettenmaier,](#)  
1083 [D. P., Riley, W. J., Singarayer, J. S., Subin, Z. M., Tian, H., Zurcher, S., Brovkin, V., van](#)  
1084 [Bodegom, P. M., Kleinen, T., Yu, Z. C. and Kaplan, J. O.: Present state of global wetland](#)  
1085 [extent and wetland methane modelling: conclusions from a model inter-comparison project](#)  
1086 [\(WETCHIMP\), \*Biogeosciences\*, 10, 2, 753-788, doi:10.5194/bg-10-753-2013, 2013.](#)

1087 [Moore, T. R. and Roulet, N. T.: Methane Flux - Water-Table Relations in Northern Wetlands,](#)  
1088 [\*Geophys. Res. Lett.\*, 20, 7, 587-590, doi:10.1029/93gl00208, 1993.](#)

1089 [Moore, T. R. and Dalva, M.: The Influence of Temperature and Water-Table Position on](#)  
1090 [Carbon-Dioxide and Methane Emissions from Laboratory Columns of Peatland Soils, \*J. Soil\*](#)  
1091 [\*Sci.\*, 44, 4, 651-664, doi:10.1111/j.1365-2389.1993.tb02330.x, 1993.](#)

1092 [Nash, J. E. and Sutcliffe, J. V.: River flow forecasting through conceptual models part I — A](#)  
1093 [discussion of principles, \*J. Hydrol.\*, 10, 3, 282–290, doi:10.1016/0022-1694\(70\)90255-6,](#)  
1094 [1970.](#)

1095 [Regina, K., Nykänen, H., Silvola, J. and Martikainen, P. J.: Fluxes of nitrous oxide from](#)  
1096 [boreal peatlands as affected by peatland type, water table level and nitrification capacity,](#)  
1097 [\*Biogeochemistry\*, 35, 401-418, doi:10.1007/BF02183033, 1996.](#)

1098 [Ridgeway, G.: Generalized boosted regression models. Documentation on the R Package](#)  
1099 [‘gbm’, version 2.1, <http://cran.r-project.org/web/packages/gbm/gbm.pdf>, accessed February](#)  
1100 [2014., 2013.](#)

1101 [Roßkopf, N., Fell, H. and Zeitz, J.: Organic soils in Germany, their distribution and carbon](#)  
1102 [stocks, \*Catena\*, submitted.](#)

1103 [Sutanudjaja, E. H., van Beek, L. P. H., de Jong, S. M., van Geer, F. C. and Bierkens, M. F. P.:](#)  
1104 [Using ERS spaceborne microwave soil moisture observations to predict groundwater head in](#)  
1105 [space and time, \*Remote sens. environ.\*, 138, 172–188, doi:10.1016/j.rse.2013.07.022, 2013.](#)

- 1106 [Tetzlaff, B., Kuhr, P. and Wendland, F.: A New Method for Creating Maps of Artificially](#)
- 1107 [Drained Areas in Large River Basins Based on Aerial Photographs and Geodata, \*Irrig. Drain.\*,](#)
- 1108 [58, 5, 569-585, doi:10.1002/Ird.426, 2009.](#)
- 1109 [Thompson, J. R., Gavin, H., Refsgaard, A., Sorenson, H. R. and Gowing, D. J.: Modelling the](#)
- 1110 [hydrological impacts of climate change on UK lowland wet grassland, \*Wetl. Ecol. Manag.\*,](#)
- 1111 [17, 5, 503-523, doi:10.1007/s11273-008-9127-1, 2009.](#)
- 1112 [UBA: National Inventory Report for the German Greenhouse Gas Inventory 1990 - 2008,](#)
- 1113 [Submission under the United Nations Framework Convention on Climate Change and the](#)
- 1114 [Kyoto Protocol 2012, Dessau, Germany, 2012.](#)
- 1115 [van den Akker, J. J. H., Jansen, P. C., Hendriks, R. F. A., Hoving, I. and Pleijter, M.:](#)
- 1116 [Submerged infiltration to halve subsidence and GHG emissions of agricultural peat soils,](#)
- 1117 [Proceedings of the 14th International Peat Congress, Stockholm, Sweden, 2012.](#)
- 1118 [van der Gaast, J. W. J., Massop, H. T. L. and Vroon, H. R. J.: Actuele grondwaterstandsituatie](#)
- 1119 [in natuurgebieden: Een. Pilotstudie, Wettelijke Onderzoekstaken Natuur & Milieu, WO-](#)
- 1120 [rapport, 94, Wageningen, 94, 2009.](#)
- 1121 [van der Ploeg, M. J., Appels, W. M., Cirkel, D. G., Oosterwoud, M. R., Witte, J. P. M. and](#)
- 1122 [van der Zee, S. E. A. T. M.: Microtopography as a Driving Mechanism for Ecohydrological](#)
- 1123 [Processes in Shallow Groundwater Systems, \*Vadose Zone J.\*, 11, 3, 52-62,](#)
- 1124 [doi:10.2136/Vzj2011.0098, 2012.](#)
- 1125 [Wackernagel, H.: Multivariate Geostatistics, Springer, Berlin, Germany, 387 pp., 2003.](#)

**Formatiert:** Einzug: Links: 0 cm,  
Hängend: 1,27 cm

**Gelöscht:** Bartholomeus, R., Witte, J. P. M., van Bodegom, P. M. and Aerts, R.: The need of data harmonization to derive robust empirical relationships between soil conditions and vegetation, *J. Veg. Sci.*, 19, 799-808, doi:10.3170/2008-8-18450, 2008.¶

Berglund, O. and Berglund, K.: Influence of water table level and soil properties on emissions of greenhouse gases from cultivated peat soil, *Soil Biol. Biochem.*, 43, 5, 923-931, doi:10.1016/j.soilbio.2011.01.002, 2011.¶

Beven, K. J. and Kirby, M.: A physically based variable contributing area model of catchment hydrology, *Hydrol. Sci. Bull.*, 24, 43-69, 1979.¶

Bierkens, M. F. P. and Stroet, C. B. M. T.: Modelling non-linear water table dynamics and specific discharge through landscape analysis, *J. Hydrol.*, 332, 3-4, 412-426, doi:10.1016/j.jhydrol.2006.07.011, 2007.¶

Bierkens, M. F. P., Knotters, M. and van Geer, F. C.: Calibration of transfer function-noise models to sparsely or irregularly observed time series, *Water Resour. Res.*, 35, 6, 1741-1750, doi:10.1029/1999wr900083, 1999.¶

Buchanan, S. and Triantafyllis, J.: Mapping Water Table Depth Using Geophysical and Environmental Variables, *Groundwater*, 47, 1, 80-96, doi:10.1111/j.1745-6584.2008.00490.x, 2009.¶

Clapcott, J., Young, R., Goodwin, E., Leathwick, J. and Kelly, D.: Relationships between multiple land-use pressures and individual and combined indicators of stream ecological integrity, Department of Conservation, DOC Research and Development series 326, Wellington, New Zealand, 2011.¶

De'ath, G.: Boosted trees for ecological modeling and prediction, *Ecology*, 88, 1, 243-251, doi:10.1890/0012-9658(2007)88[243:Btfema]2.0.Co;2, 2007.¶

Dormann, C. F., Elith, J., Bacher, S., Buchmann, C., Carl, G., Carre, G., Marquez, J. R. G., Gruber, B., Lafourcade, B., Leitao, P. J., Munkemüller, T., McClean, C., Osborne, P. E., Reineking, B., Schroder, B., Skidmore, A. K., Zurell, D. and Lautenbach, S.: Collinearity: a review of methods to deal with it and a simulation study evaluating their performance, *Ecography*, 36, 1, 27-46, doi:10.1111/j.1600-0587.2012.07348.x, 2013.¶

Drösler, M., Freibauer, A., Adelman, W., Augustin, J., Bergmann, L., Beyer, C., Chojnicki, B., Förster, C., Giebels, M., Görlitz, S., Höper, H., Kantelhardt, J., Liebersbach, H., Hahn-Schöfl, M., Minke, M., Petschow, U., Pfadenhauer, J., Schaller, L., Schägner, P., Sommer, M., Thuille, A. and Wehrhan, M.: Klimaschutz durch Moorschutz in der Praxis, Ergebnisse aus dem BMBF-Verbundprojekt „Klimaschutz - Moornutzungsstrategien“ 2006-2010, vTI-Arbeitsberichte 4/2011, 2011.¶

Elith, J., Leathwick, J. R. and Hastie, T.: A working guide to boosted regression trees, *J. Anim. Ecol.*, 77, 4, 802-813, ... [1]

1 Table 1. Overview on predictor variables.

Predictor Variable	Variable name	Values	Point/Buffers (m)	Data Source
Land use type		Arable, grassland, forest, shrubs, peat-mining, unused peatland, swamp, open water	point, 100, 500, 1000, 2500	Digital Landscape Model <sup>1</sup>
Vegetation attributes (optional)		Deciduous forest, mixed forest, coniferous forest, reed, shrubs, grass	point	Digital Landscape Model <sup>1</sup>
'Wet soil observed'		Yes, no	point	Digital Landscape Model <sup>1</sup>
Combined land cover information (land use type + veg. + wet soil attr.)	lc	Arable, grassland, wet grassland, deciduous including mixed forest, wet forest, coniferous forest, reed, unused peatland, wet unused peatland	point, 100, 500, 1000, 2500	Digital Landscape Model <sup>1</sup>
Dry land cover fraction	$f_{dry}(X)$	arable + 0.5*grassland on organic soil area; 0 to 1	100, 500, 1000, 2500	Digital Landscape Model <sup>1</sup>
Wet land cover fraction		reed+ wet grassland+wet forest+wet unused peatland on organic soil area; 0 to 1	100, 500, 1000, 2500	Digital Landscape Model <sup>1</sup>
Total length of ditches for all lc and only for arable and grassland (subscr.: 'dry')	$di_{len,dry}(X)$	$\geq 0$ m	point, 50, 250, 1000, 2500	Digital Landscape Model <sup>1</sup>
Distance to next ditch		$\geq 0$ m	point	Digital Landscape Model <sup>1</sup>
Peatland type	$p_{type}$	Lowland bog, upland bog, fen neighboring surface water, fen without neighboring surface water, other 'low-C' organic soil	point	Map of organic soils <sup>2</sup>
Material at peat base	$p_{base}$	Unconsolidated rock, peat clay layer, rock, no information	point	Map of organic soils <sup>2</sup>
Peatland fraction	$f_{peat}(X)$	0 to 1	point, 500, 1000, 2500	Geological Map (BGR) <sup>3</sup>
Distance to edge of peatland		$> 0$ m		Geological Map (BGR) <sup>3</sup>
Ratio of $d_{peat}/f_{peat}$		$> 0$	2500	Geological Map (BGR) <sup>3</sup>
Precipitation		$\geq 0$ mm	point	raster map 1x1km (DWD) <sup>4</sup>
Evapotranspiration		$\geq 0$ mm	point	raster map 1x1km (DWD) <sup>4</sup>
Climatic water balance	$wb_{summer}$	$< 0$ and $\geq 0$ mm	point	raster map 1x1km (DWD) <sup>4</sup>
Relative height	$h_{rel}(X)$	$< 0$ and $\geq 0$ m	point - median 25, 50, 100, 250, 500, 1000	Digital Elevation Model <sup>5</sup>
Topographic index	$ti_{rasR}(X)$	$> 0$	point and 1000 buffer for 10, 25, 250, 1000 raster values	Digital Elevation Model <sup>5</sup>
Protection status		Nature Conservation Area, Special Areas of Conservation, Special Protection Area for wild birds, UNESCO-biosphere reserve, Nature Park, National Park, Landscape Protection Area	point	Maps of protected areas <sup>6</sup>

2 | <sup>1</sup> ATKIS Basis DLM, Federal Agency for Cartography and Geodesy, BKG; <sup>2</sup> Map of organic soils (Roßkopf et al., submitted, Humboldt University of Berlin); <sup>3</sup> Geological Map 1:200 000  
3 | (GUEK 200, BGR - Federal Institute for Geosciences and Natural Resources); <sup>4</sup> raster map 1x1 km of weather data (German Weather Service); <sup>5</sup> BKG; Variable name indicated for the nine  
4 | variables in the final model with (X) indicating buf. size and R indicating raster resolution. <sup>6</sup> Federal Agency for Nature Conservation (BfN)

Gelöscht: Roßkopf et al., submitted

1 Table 2. Weighted mean and standard deviation of WL and WL<sub>t</sub> data, and of the WL<sub>t</sub> map  
 2 presented in section 3.6, for the nine land cover classes.

	WL (m) mean ± sd	WL <sub>t</sub> (-) mean ± sd	WL <sub>t</sub> (-), map mean ± sd
arable land	-0.69±0.30	-0.76±0.17	-0.66±0.22
deciduous f.	-0.45±0.34	-0.49±0.37	-0.47±0.35
grassland	-0.44±0.29	-0.52±0.32	-0.49±0.30
unused peatl.	-0.39±0.36	-0.39±0.41	-0.37±0.40
coniferous f.	-0.36±0.36	-0.37±0.37	-0.46±0.35
wet unused peatl.	-0.22±0.27	-0.18±0.40	-0.17±0.36
wet forest	-0.22±0.29	-0.17±0.43	-0.21±0.39
wet grassland	-0.10±0.14	-0.00±0.31	-0.15±0.39
reed	-0.01±0.17	0.20±0.29	-0.06±0.32

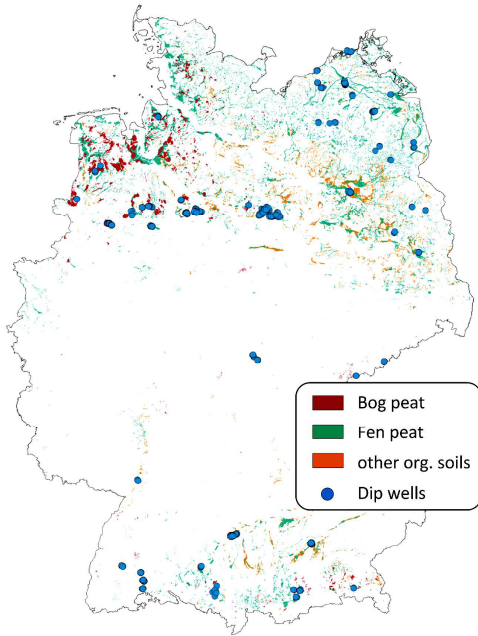
3

1  
 2 Table 3. Performance criteria of the different models; dry range defined as  $WL < -0.3$  m and  
 3 wet range as  $WL > -0.3$  m.

	WL (m) (calibrated on WL)	WL <sub>t</sub> (-) (calibrated on WL)	WL <sub>t</sub> (-) (calibrated on WL <sub>t</sub> )
NSE <sub>cal</sub>	0.627	0.559	0.642
NSE <sub>cv</sub>	0.381	0.397	0.453
RMSE <sub>cv</sub>	0.269	0.299	0.284
RMSE <sub>cv,dry</sub>	0.284	0.263	0.259
RMSE <sub>cv,wet</sub>	0.222	0.382	0.355
Bias	-0.003	0.083	0.002
Bias <sub>dry</sub>	-0.012	0.070	0.003
Bias <sub>wet</sub>	0.021	0.120	0.000

4  
 5

1

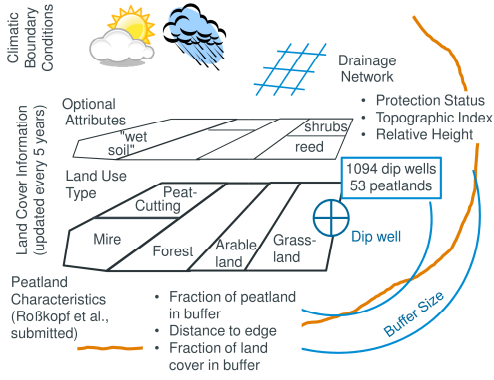


2

3 Figure 1. Locations of the 1094 dip wells of the dataset. Base map (Geological map  
4 1:200,000, BGR) shows the distribution of bog and fen peat, and other organic soils.

5

1

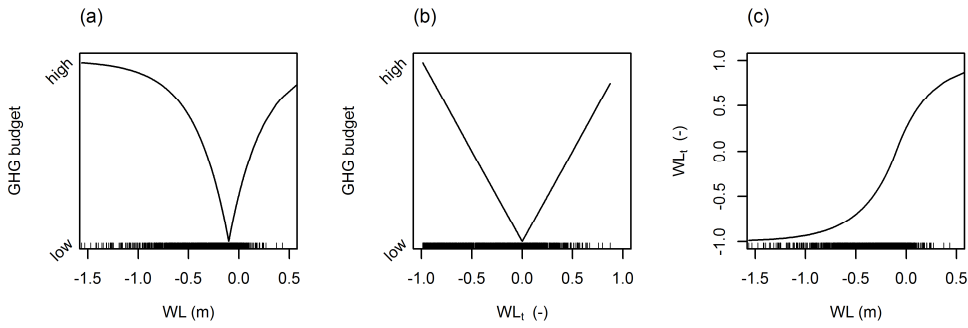


2

3 Figure 2. Illustration of the predictor variables determined for each dip well based on  
4 available national maps (see Table 1).

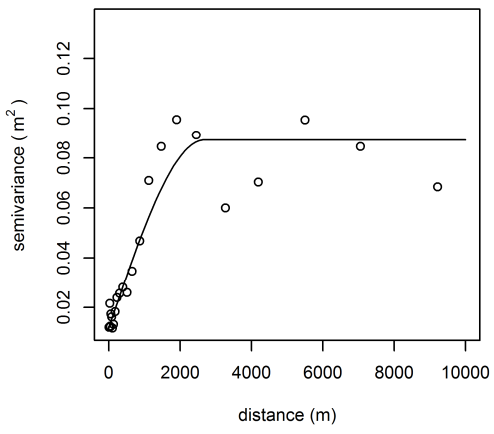
5

1



2  
3 Figure 3. Illustration of the annual mean water level (WL) transformation. (a) Hypothetical  
4 transfer function relating GHG budget to WL (m). (b) GHG budget vs. the transformed water  
5 level (WL<sub>t</sub>). (c) WL<sub>t</sub> vs. WL. Rugs indicate the data quantiles of the analyzed dataset.

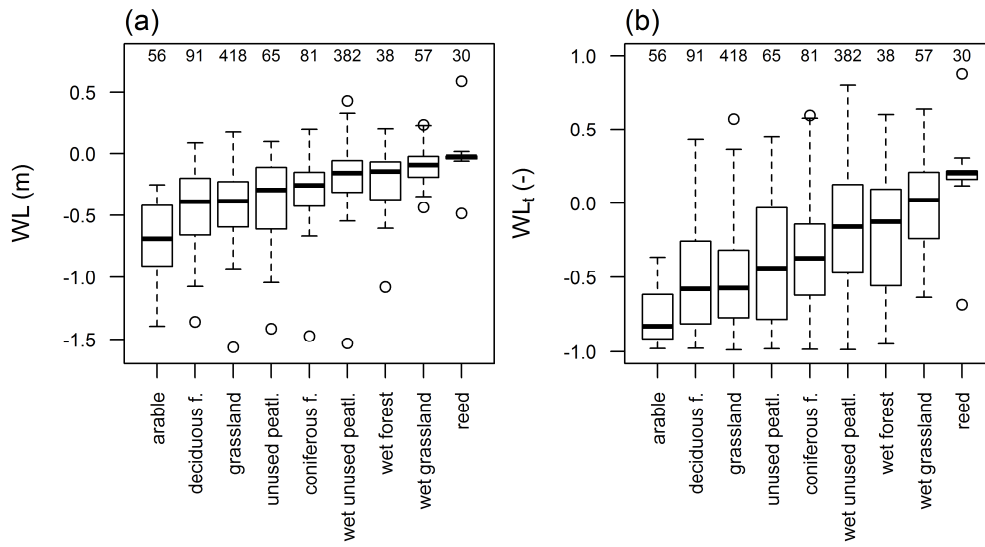
6  
7  
8



1  
2 Figure 4. Sample semi-variogram and fitted semi-variogram model of the annual mean water  
3 level data, WL.  
4  
5

1

2



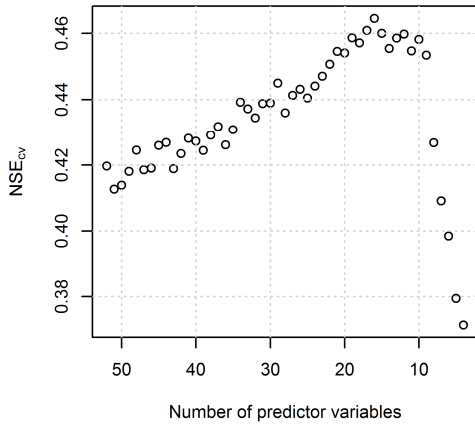
3

4

5 Figure 5. Water level relative to ground surface, WL (m), and transformed water level,  
6 WL<sub>t</sub> (-), by land cover class illustrated as weighted box plot. WL<sub>t</sub> = -1 corresponds to  
7 maximum CO<sub>2</sub> emissions and WL<sub>t</sub> = 1 to maximum CH<sub>4</sub> emissions. In the upper part, the  
8 number of dip wells in each class is indicated.

9

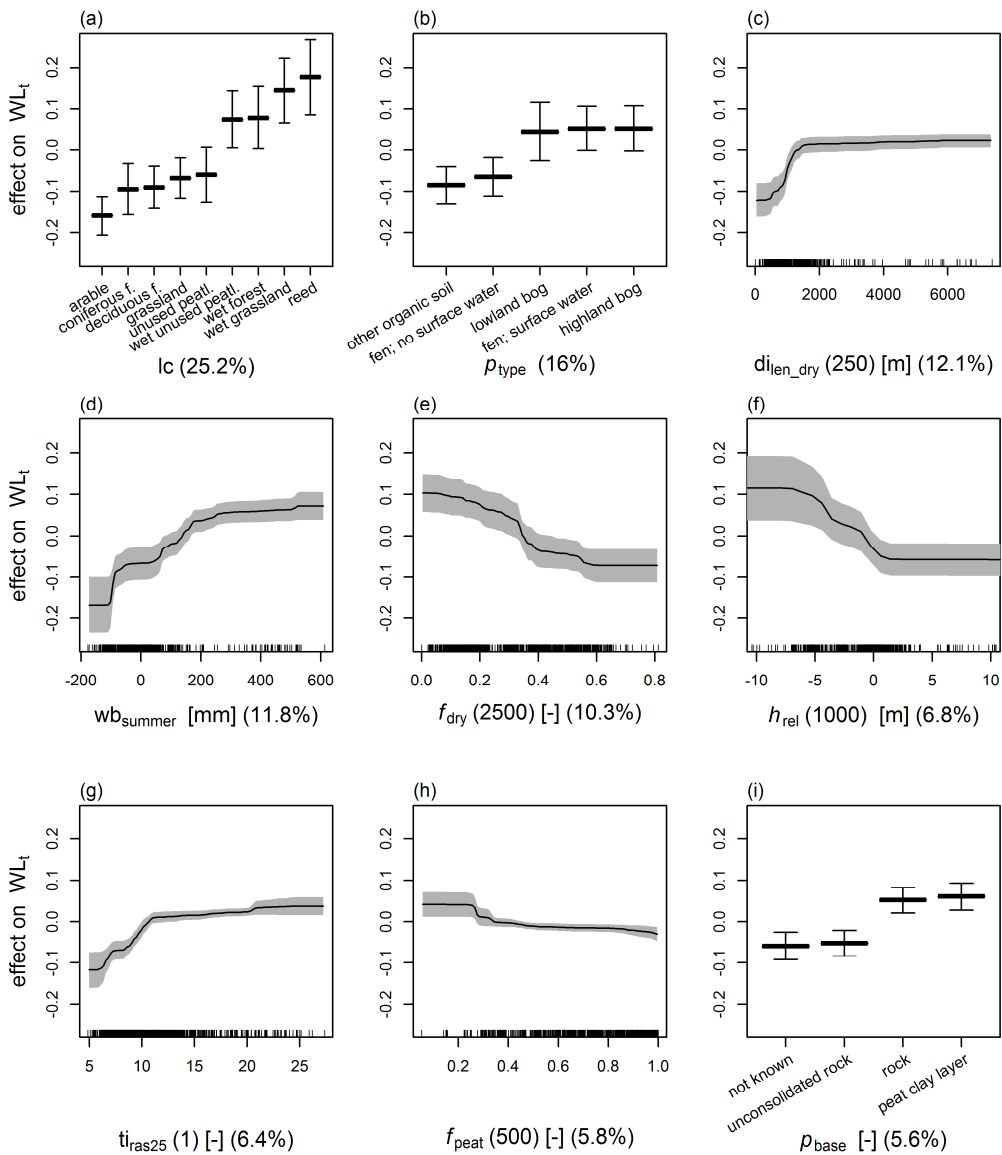
1



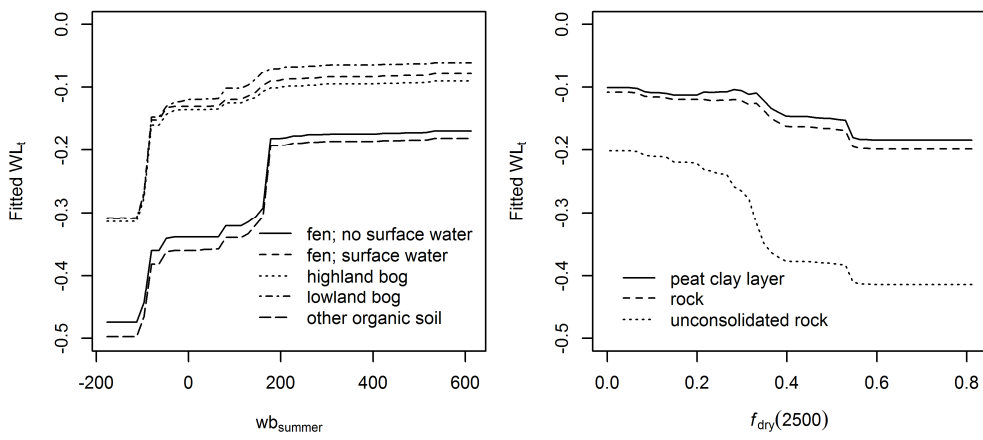
2

3 Figure 6.  $NSE_{cv}$  as a function of number of predictor variables used in the model of  $WL_t$   
4 during model simplification and shown for the last 50 parameter drops.

5



1  
2 Figure 7. Partial dependence plots for the predictor variables. For explanation of variables see  
3 Table 1. Y axes are on  $WL_t$  scale and are centered around the mean  $WL_t$ . Error bars and grey  
4 area indicate standard deviation of the response over 1000 bootstrap models. The relative  
5 contribution of each predictor is indicated as percentage. Rugs at bottom of each plot show  
6 distribution of data across that variable, in deciles.

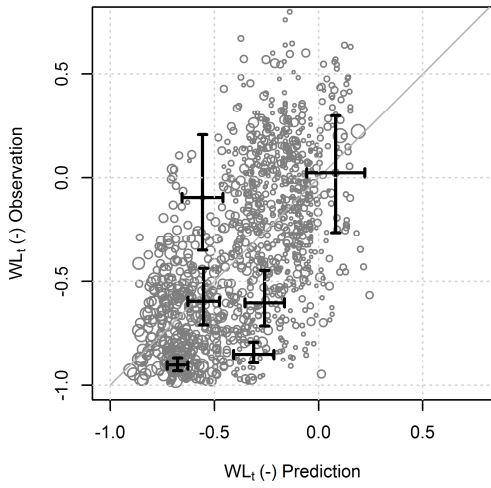


1  
 2 Figure 8. Partial dependence plots representing the two strongest interactions in the model: (a)  
 3 between  $p_{type}$  and  $wb_{summer}$  and (b) between  $p_{base}$  and  $f_{dry}$ . Fitted  $WL_t$  is plotted on the y-axis  
 4 which is obtained after accounting for the average effect of all other predictor variables.

5  
 6

1

2

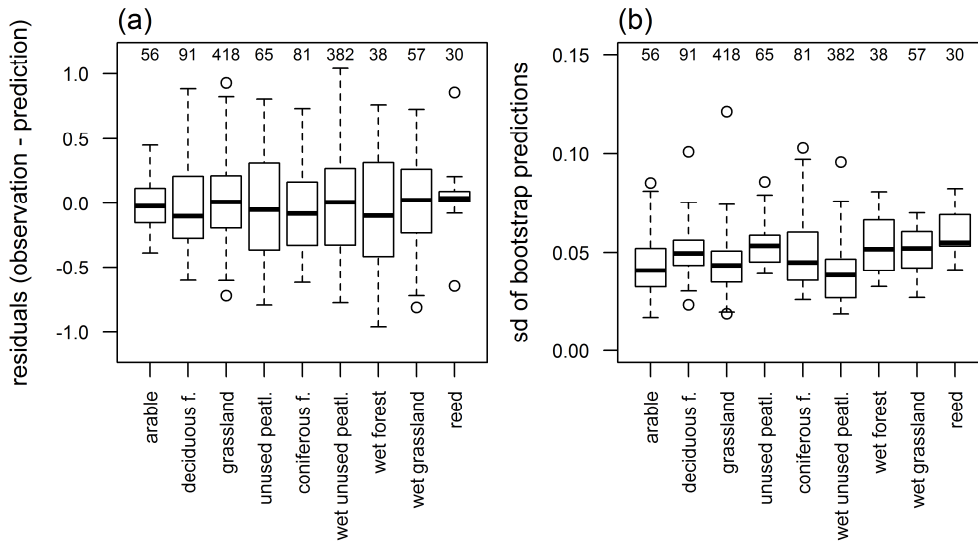


3

4 Figure 9. Observed vs. predicted transformed annual mean water level ( $WL_t$ ) from cross-  
5 validation results. Error bars show selected data and bootstrap model errors as standard  
6 deviation. Data points are scaled by their weights.

7

1

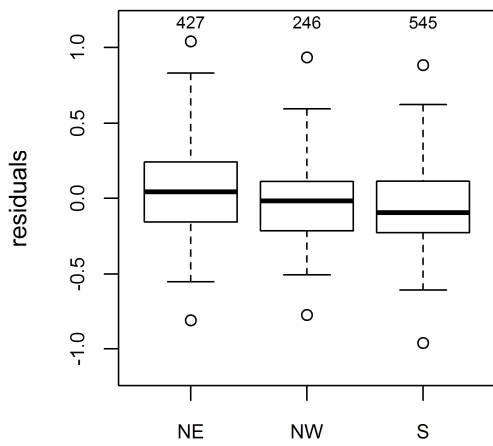


2

3 Figure 10. (a) Residuals (observation - prediction) of  $WL_t$  predictions and (b) standard  
4 deviation (sd) of bootstrap predictions shown for the nine land cover classes. In the upper  
5 part, the number of dip wells in each class is indicated.

6

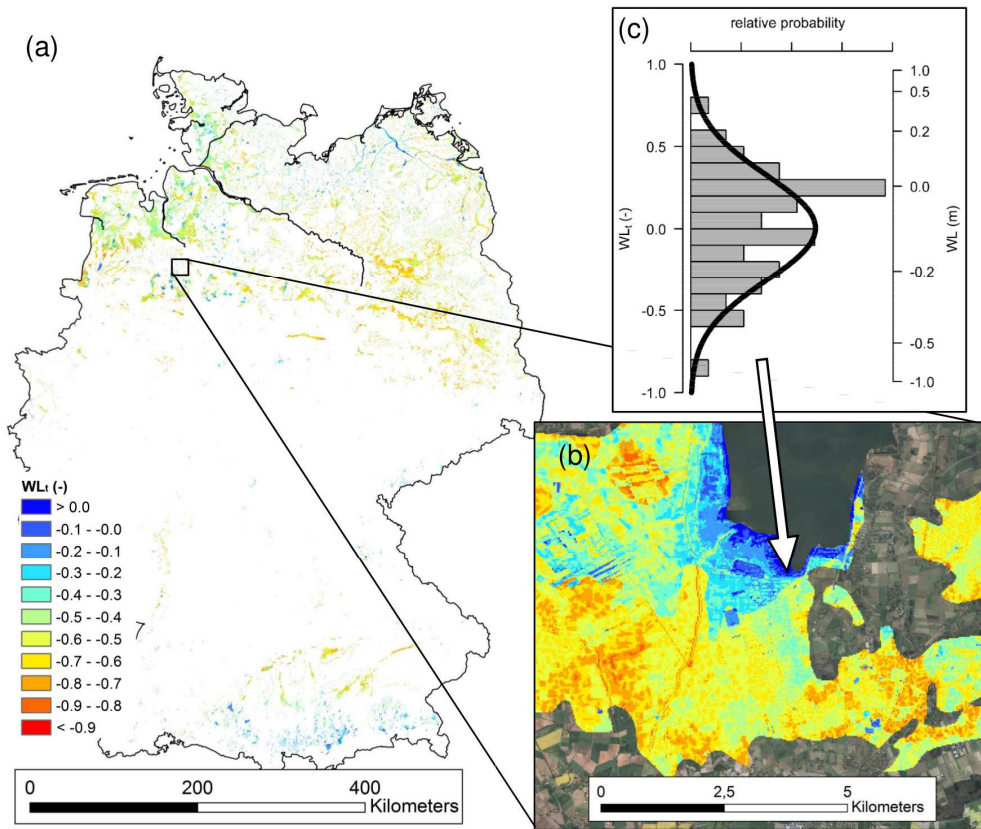
7



1  
 2 Figure 11. Residuals (observation - prediction) of  $WL_t$  predictions for the three major  
 3 geographical peatland regions of Germany. In the upper part, the number of dip wells in each  
 4 class is indicated.

5  
 6

1



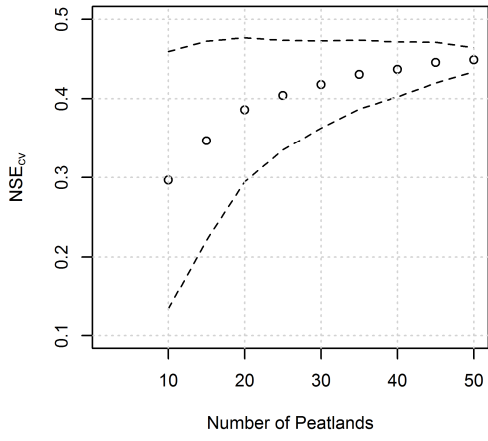
2

3

4 Figure 12. Map of predictions of transformed annual mean water level ( $WL_t$ ) for all German  
5 organic soils (a) and an enlarged map section (b). Probability distribution in (c) exemplarily  
6 indicates the uncertainty of a specific point prediction for wet grassland. Here, predicted value  
7 is approximately  $WL_t=0$ , but note that wet grassland predictions do vary in space depending  
8 on the values of the other model parameter. The histogram shows the residuals from cross-  
9 validation for wet grassland, to which the probability distribution was fitted.

10

1



2

3

4 Figure 13. NSE of cross-validation vs. number of randomly selected peatland areas. Dashed  
5 lines indicate  $NSE_{cv} \pm$  standard deviation.

Bartholomeus, R., Witte, J. P. M., van Bodegom, P. M. and Aerts, R.: The need of data harmonization to derive robust empirical relationships between soil conditions and vegetation, *J. Veg. Sci.*, 19, 799-808, doi:10.3170/2008-8-18450, 2008.

Berglund, O. and Berglund, K.: Influence of water table level and soil properties on emissions of greenhouse gases from cultivated peat soil, *Soil Biol. Biochem.*, 43, 5, 923-931, doi:10.1016/j.soilbio.2011.01.002, 2011.

Beven, K. J. and Kirby, M.: A physically based variable contributing area model of catchment hydrology, *Hydrol. Sci. Bull.*, 24, 43-69, 1979.

Bierkens, M. F. P. and Stroet, C. B. M. T.: Modelling non-linear water table dynamics and specific discharge through landscape analysis, *J. Hydrol.*, 332, 3-4, 412-426, doi:10.1016/j.jhydrol.2006.07.011, 2007.

Bierkens, M. F. P., Knotters, M. and van Geer, F. C.: Calibration of transfer function-noise models to sparsely or irregularly observed time series, *Water Resour. Res.*, 35, 6, 1741-1750, doi:10.1029/1999wr900083, 1999.

Buchanan, S. and Triantafilis, J.: Mapping Water Table Depth Using Geophysical and Environmental Variables, *Groundwater*, 47, 1, 80-96, doi:10.1111/j.1745-6584.2008.00490.x, 2009.

Clapcott, J., Young, R., Goodwin, E., Leathwick, J. and Kelly, D.: Relationships between multiple land-use pressures and individual and combined indicators of stream ecological integrity, Department of Conservation, DOC Research and Development series 326, Wellington, New Zealand, 2011.

De'ath, G.: Boosted trees for ecological modeling and prediction, *Ecology*, 88, 1, 243-251, doi:10.1890/0012-9658(2007)88[243:Btfema]2.0.Co;2, 2007.

Dormann, C. F., Elith, J., Bacher, S., Buchmann, C., Carl, G., Carre, G., Marquez, J. R. G., Gruber, B., Lafourcade, B., Leitao, P. J., Munkemuller, T., McClean, C., Osborne, P. E., Reineking, B., Schroder, B., Skidmore, A. K., Zurell, D. and Lautenbach, S.: Collinearity: a review of methods to deal with it and a simulation study evaluating their performance, *Ecography*, 36, 1, 27-46, doi:10.1111/j.1600-0587.2012.07348.x, 2013.

Drösler, M., Freibauer, A., Adelman, W., Augustin, J., Bergmann, L., Beyer, C., Chojnicki, B., Förster, C., Giebels, M., Görlitz, S., Höper, H., Kantelhardt, J., Liebersbach, H., Hahn-Schöfl, M., Minke, M., Petschow, U., Pfadenhauer, J., Schaller, L., Schägner, P., Sommer,

- M., Thuille, A. and Wehrhan, M.: Klimaschutz durch Moorschutz in der Praxis, Ergebnisse aus dem BMBF-Verbundprojekt „Klimaschutz - Moornutzungsstrategien“ 2006-2010, vTI-Arbeitsberichte 4/2011, 2011.
- Elith, J., Leathwick, J. R. and Hastie, T.: A working guide to boosted regression trees, *J. Anim. Ecol.*, 77, 4, 802-813, doi:10.1111/j.1365-2656.2008.01390.x, 2008.
- Fan, Y. and Miguez-Macho, G.: A simple hydrologic framework for simulating wetlands in climate and earth system models, *Clim. Dynam.*, 37, 1-2, 253-278, doi:10.1007/s00382-010-0829-8, 2011.
- Fell, H., Roßkopf, N. and Zeitz, J.: Organic soils in Germany, their distribution and carbon stocks, *Catena*, in prep.
- Finke, P. A., Brus, D. J., Bierkens, M. F. P., Hoogland, T., Knotters, M. and de Vries, F.: Mapping groundwater dynamics using multiple sources of exhaustive high resolution data, *Geoderma*, 123, 1-2, 23-39, doi:10.1016/j.geoderma.2004.01.025, 2004.
- Gong, J. N., Wang, K. Y., Kellomaki, S., Zhang, C., Martikainen, P. J. and Shurpali, N.: Modeling water table changes in boreal peatlands of Finland under changing climate conditions, *Ecol. Model.*, 244, 65-78, doi:10.1016/j.ecolmodel.2012.06.031, 2012.
- Hahn-Schöfl, M., Zak, D., Minke, M., Gelbrecht, J., Augustin, J. and Freibauer, A.: Organic sediment formed during inundation of a degraded fen grassland emits large fluxes of CH<sub>4</sub> and CO<sub>2</sub>, *Biogeosciences*, 8, 6, 1539-1550, doi:10.5194/bg-8-1539-2011, 2011.
- Hijmans, R. J.: Species distribution modeling. Documentation on the R Package ‘dismo’, version 0.9-3, <http://cran.r-project.org/web/packages/dismo/dismo.pdf>, accessed February 2014, 2013.
- Hoogland, T., Heuvelink, G. B. M. and Knotters, M.: Mapping Water-Table Depths Over Time to Assess Desiccation of Groundwater-Dependent Ecosystems in the Netherlands, *Wetlands*, 30, 1, 137-147, doi:10.1007/s13157-009-0011-4, 2010.
- IPCC: IPCC guidelines for national greenhouse gas inventories, In: Eggleston, H.S., Buendia, L., Miwa, K., Ngara, T., K., T. (Eds.). IGES, Japan, 2006.
- Ju, W. M., Chen, J. M., Black, T. A., Barr, A. G., Mccaughey, H. and Roulet, N. T.: Hydrological effects on carbon cycles of Canada's forests and wetlands, *Tellus B*, 58, 1, 16-30, doi:10.1111/j.1600-0889.2005.00168.x, 2006.

Knotters, M. and van Walsum, P. E. V.: Estimating fluctuation quantities from time series of water-table depths using models with a stochastic component, *J. Hydrol.*, 197, 1-4, 25-46, doi:10.1016/S0022-1694(96)03278-7, 1997.

Leathwick, J. R., Elith, J., Francis, M. P., Hastie, T. and Taylor, P.: Variation in demersal fish species richness in the oceans surrounding New Zealand: an analysis using boosted regression trees, *Mar. Ecol. Prog. Ser.*, 321, 267-281, doi:10.3354/Meps321267, 2006.

Leiber-Sauheitl, K., Fuß, R., Voigt, C. and Freibauer, A.: High CO<sub>2</sub> fluxes from grassland on histic Gleysol along soil carbon and drainage gradients, *Biogeosciences*, 11, 735-747, doi:10.5194/bg-11-749-2014, 2014.

Levy, P. E., Burden, A., Cooper, M. D. A., Dinsmore, K. J., Drewer, J., Evans, C., Fowler, D., Gaiawyn, J., Gray, A., Jones, S. K., Jones, T., Mcnamara, N. P., Mills, R., Ostle, N., Sheppard, L. J., Skiba, U., Sowerby, A., Ward, S. E. and Zielinski, P.: Methane emissions from soils: synthesis and analysis of a large UK data set, *Global change biology*, 18, 5, 1657-1669, doi:10.1111/j.1365-2486.2011.02616.x, 2012.

Limpens, J., Berendse, F., Blodau, C., Canadell, J. G., Freeman, C., Holden, J., Roulet, N., Rydin, H. and Schaepman-Strub, G.: Peatlands and the carbon cycle: from local processes to global implications - a synthesis, *Biogeosciences*, 5, 5, 1475-1491, doi:10.5194/bg-5-1475-2008, 2008.

Martin, M. P., Wattenbach, M., Smith, P., Meersmans, J., Jolivet, C., Boulonne, L. and Arrouays, D.: Spatial distribution of soil organic carbon stocks in France, *Biogeosciences*, 8, 5, 1053-1065, doi:10.5194/bg-8-1053-2011, 2011.

Melton, J. R., Wania, R., Hodson, E. L., Poulter, B., Ringeval, B., Spahni, R., Bohn, T., Avis, C. A., Beerling, D. J., Chen, G., Eliseev, A. V., Denisov, S. N., Hopcroft, P. O., Lettenmaier, D. P., Riley, W. J., Singarayer, J. S., Subin, Z. M., Tian, H., Zurcher, S., Brovkin, V., van Bodegom, P. M., Kleinen, T., Yu, Z. C. and Kaplan, J. O.: Present state of global wetland extent and wetland methane modelling: conclusions from a model inter-comparison project (WETCHIMP), *Biogeosciences*, 10, 2, 753-788, doi:10.5194/bg-10-753-2013, 2013.

Moore, T. R. and Dalva, M.: The Influence of Temperature and Water-Table Position on Carbon-Dioxide and Methane Emissions from Laboratory Columns of Peatland Soils, *J. Soil Sci.*, 44, 4, 651-664, doi:10.1111/j.1365-2389.1993.tb02330.x, 1993.

Moore, T. R. and Roulet, N. T.: Methane Flux - Water-Table Relations in Northern Wetlands, *Geophys. Res. Lett.*, 20, 7, 587-590, doi:10.1029/93gl00208, 1993.

Nash, J. E. and Sutcliffe, J. V.: River flow forecasting through conceptual models part I — A discussion of principles, *J. Hydrol.*, 10, 3, 282–290, doi:10.1016/0022-1694(70)90255-6, 1970.

Regina, K., Nykänen, H., Silvola, J. and Martikainen, P. J.: Fluxes of nitrous oxide from boreal peatlands as affected by peatland type, water table level and nitrification capacity, *Biogeochemistry*, 35, 401–418, doi:10.1007/BF02183033, 1996.

Ridgeway, G.: Generalized boosted regression models. Documentation on the R Package ‘gbm’, version 2.1, <http://cran.r-project.org/web/packages/gbm/gbm.pdf>, accessed February 2014., 2013.

Sutanudjaja, E. H., van Beek, L. P. H., de Jong, S. M., van Geer, F. C. and Bierkens, M. F. P.: Using ERS spaceborne microwave soil moisture observations to predict groundwater head in space and time, *Remote sens. environ.*, 138, 172–188, doi:10.1016/j.rse.2013.07.022, 2013.

Tetzlaff, B., Kuhr, P. and Wendland, F.: A New Method for Creating Maps of Artificially Drained Areas in Large River Basins Based on Aerial Photographs and Geodata, *Irrig. Drain.*, 58, 5, 569–585, doi:10.1002/Ird.426, 2009.

Thompson, J. R., Gavin, H., Refsgaard, A., Sorenson, H. R. and Gowing, D. J.: Modelling the hydrological impacts of climate change on UK lowland wet grassland, *Wetl. Ecol. Manag.*, 17, 5, 503–523, doi:10.1007/s11273-008-9127-1, 2009.

UBA: National Inventory Report for the German Greenhouse Gas Inventory 1990 - 2008, Submission under the United Nations Framework Convention on Climate Change and the Kyoto Protocol 2012, Dessau, Germany, 2012.

van der Gaast, J. W. J., Massop, H. T. L. and Vroon, H. R. J.: Actuele grondwaterstandsituatie in natuurgebieden: Een. Pilotstudie, Wettelijke Onderzoekstaken Natuur & Milieu, WOt-rapport, 94, Wageningen, 94, 2009.

van der Ploeg, M. J., Appels, W. M., Cirkel, D. G., Oosterwoud, M. R., Witte, J. P. M. and van der Zee, S. E. A. T. M.: Microtopography as a Driving Mechanism for Ecohydrological Processes in Shallow Groundwater Systems, *Vadose Zone J.*, 11, 3, 52–62, doi:10.2136/Vzj2011.0098, 2012.